Self-Assembled Monolayers on the Surface of Metal Nanoparticles

3-D SAMs

Prof. LUCIA PASQUATO

University of Trieste, Department of Chemical and Pharmaceutical Sciences

E-mail: lpasquato@units.it

Outline

- **Introduction to nanoparticles**
- **Monolayer-Protectected Metal nanoparticles**
  synthesis, characterizations
  properties and packing of the monolayer
- **Functional Nanoparticles**
  Methods of synthesis. Mixed-monolayers
  Characterization techniques
  Properties

Chem. Rev. **2005**, 105, 1103.

SCOPUS

«Nanoparticle*» ricerca del 4/11/2024

950,820 document results

Select year range to analyze: 1990 to 2025 Analyze

Year ↓	Documents ↑
2025	1359
2024	74858
2023	78633
2022	78582
2021	73753
2020	71461
2019	66849
2018	59790
2017	56211

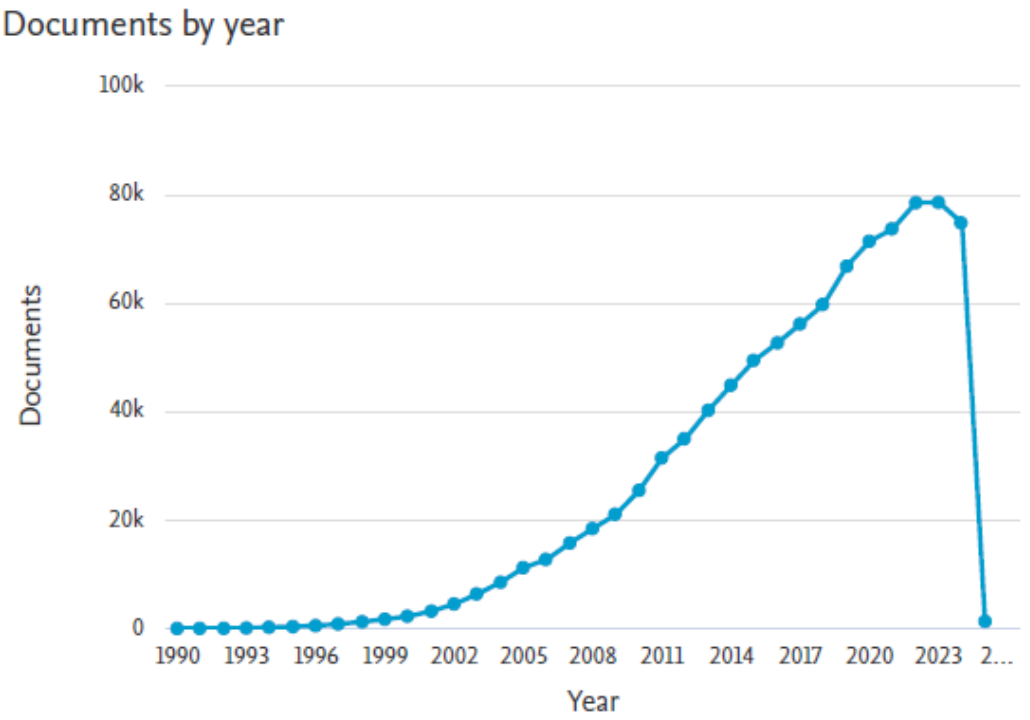

NANOMATERIALS

definition

size In the scientific community, it is commonly used to designate structures at least 1 nm but less (often much less) than 1μm. However, semantics apart, there is another requirement that is commonly accepted for inclusion in the "nanoclub"; **the structure should be artificially made**. Note that the word 'structure' is deliberately used: macromolecules, for example, can justifiably be considered to be nanomaterials, yet they are not usually so classified.

- "what is so special about nanomaterials"?

NANOMATERIALS

- What properties or behavior can nanomaterials exhibit that they would not do if they were not so small?

Table 1. Different size-related phenomena. The length scales are a rough estimation of the size below which the phenomenon can be observed (for the last three phenomenon, typical values of the sizes—screening lengths and ballistic transport in particular—can vary over orders of magnitude).

Phenomenon	Typical length scale
Size quantization	tens of nanometers
Crystal phase	tens of nanometers
Doping/defects	tens of nanometers
Single-charge effects	ca. 50 nm (at room temperature)
Charge depletion (screening length)	ca. 100 nm
Scattering/interference of light	hundreds of nanometers
Ballistic electron transport	hundreds of nanometers

A brief historical background

- gold nanoparticles are known since ancient time, 5º - 4º millenium B.C. (China, Egypt). We believe that ancient Egyptian known how to prepare "soluble" gold and they were used these solutions as "elisir".

- colloidal gold sols are used to obtain red glass

- around 1600 Paracelso (1493-1541) described the preparation of "aurum potable, oleum auri: quinta essentia auri" by reduction of acid tetrachloroauric using an alcoholic extract of plants.

  At that time medical doctors believed that "drinkable gold" exert curative properties for several diseases.

A brief historical background

The roman industry of IV century A.D., developed a sophisticated use of metal NPs, they were able to produce colored glass with particular optical properties.
For example the addition of Ag and Au compounds, enable to produce glass which appear to be green under reflected light and red under trasmitted light.
The famous "Licurgus cup" has been realized with this technique.

day light (reflected light)

trasmitted light

40 ppm of Au and 300 ppm of Ag

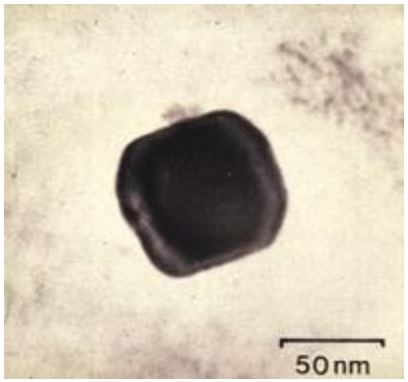

TEM image

Nanoparticles - hystorical background

- in 1857 Michael Faraday reported the first scientific studies on preparations of colloidal gold solutions, M. Faraday, *Phil.Trans.Roy. Soc.* **1857**, *147*, 145.
- around the half of 19th century the Italian physicist Enrico Selmi write a description of "colloids", not very different from the actual definition.
- in 1861 the term "**colloid**" (from the greek *kolla)* was conied by the Scottish chemist Thomas Graham

$(AuCl_4)^-$ —white phosphorous, reduction on CS_2→ solution of colloids

diameter of 3 ÷ 30 nm

two phase system

Nanoscale Materials

Florence - Santa Croce

Milan - Duomo

«The kiss» by Gustav Klimt, 1908

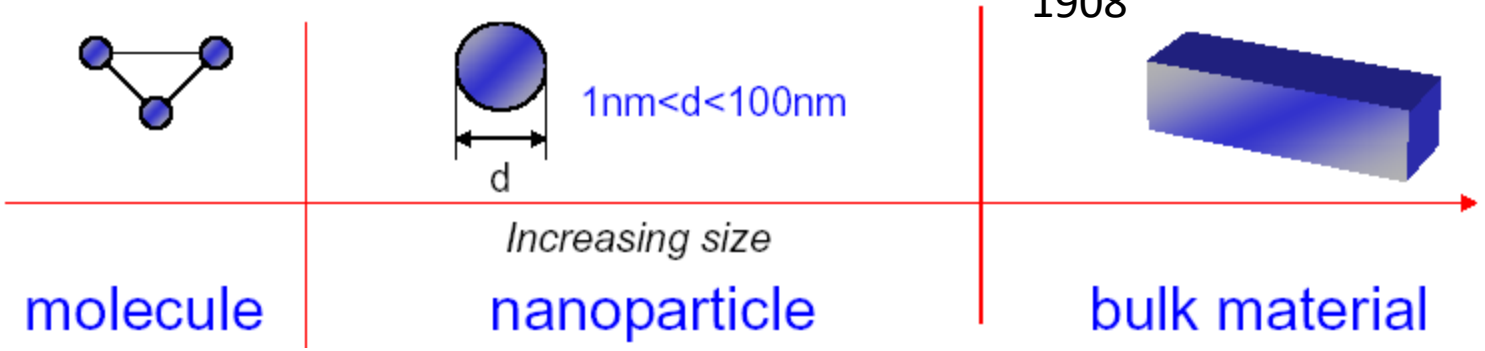

Nanoscale materials have different properties when compared to their bulk counterparts!

Nanoscale Materials

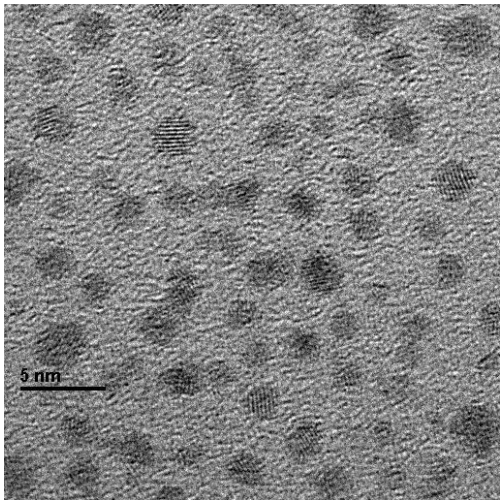

Nanoparticles - quantum dots

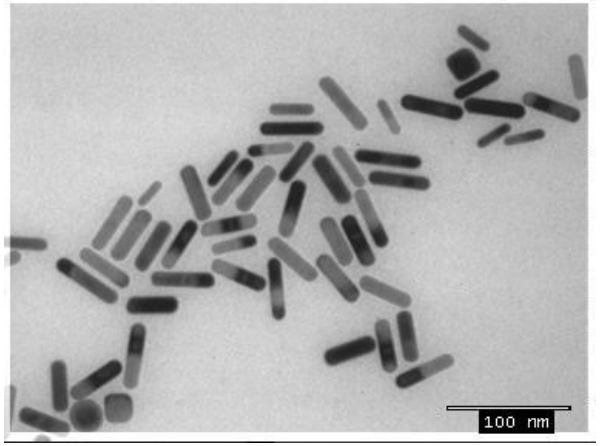

nanorods

0 dimensional nanomaterials:
unique properties due to
quantum confinement
and very high surface/volume ratio

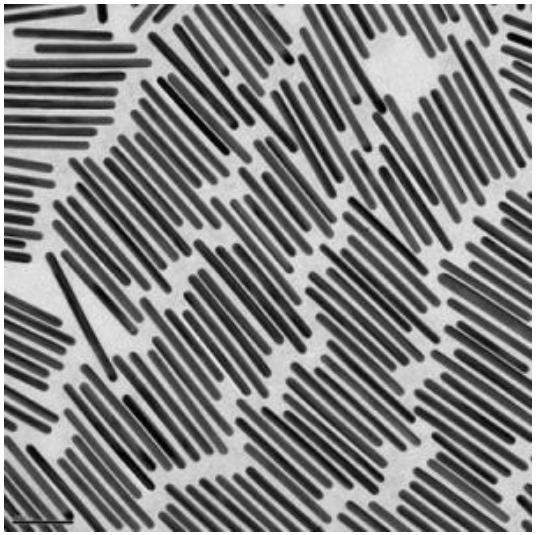

nanowires

1 dimensional nanomaterials:
extremely efficient
classical properties

These ultra-long devices exhibit tremendous photothermal properties, converting up to 90% of incident light energy to heat.

Properties of Metal Nanoparticles

Optical Properties

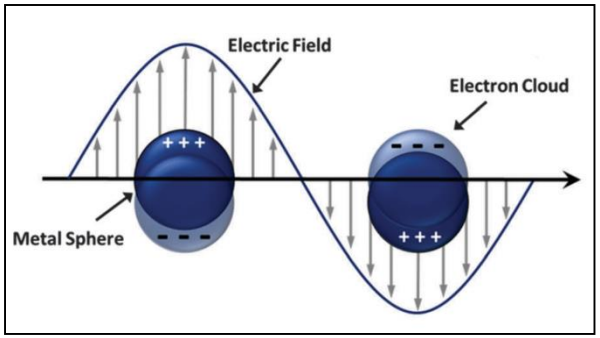

Nanoscale Materials have different properties when compared to their bulk counterparts!

Electronic Properties

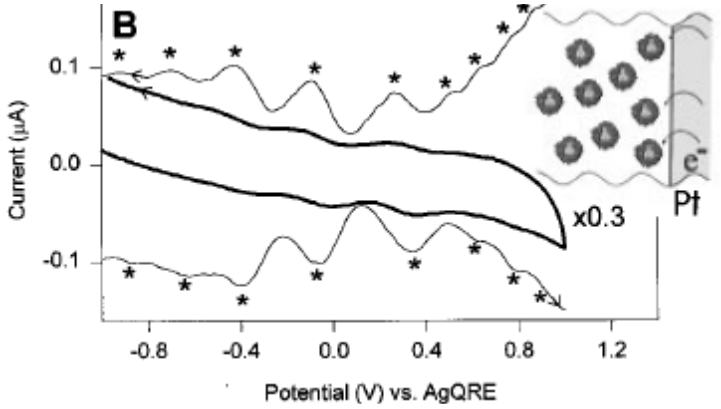

Otical properies of semiconductor NPs

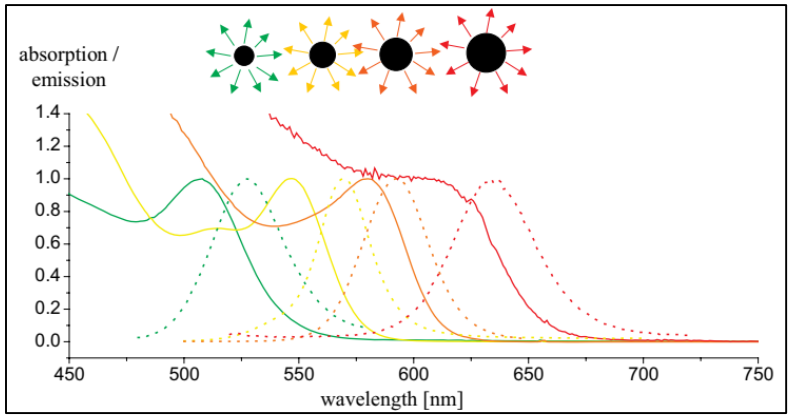

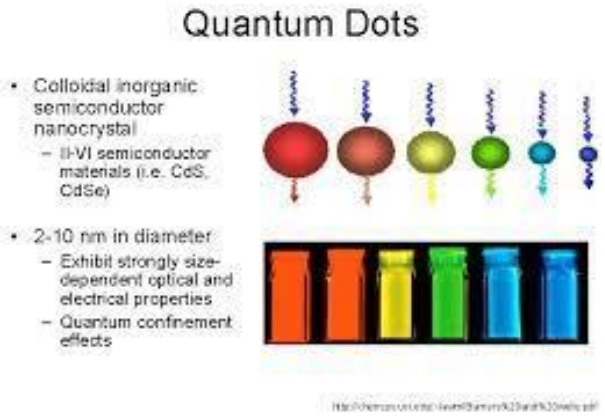

Nanoscale Materials

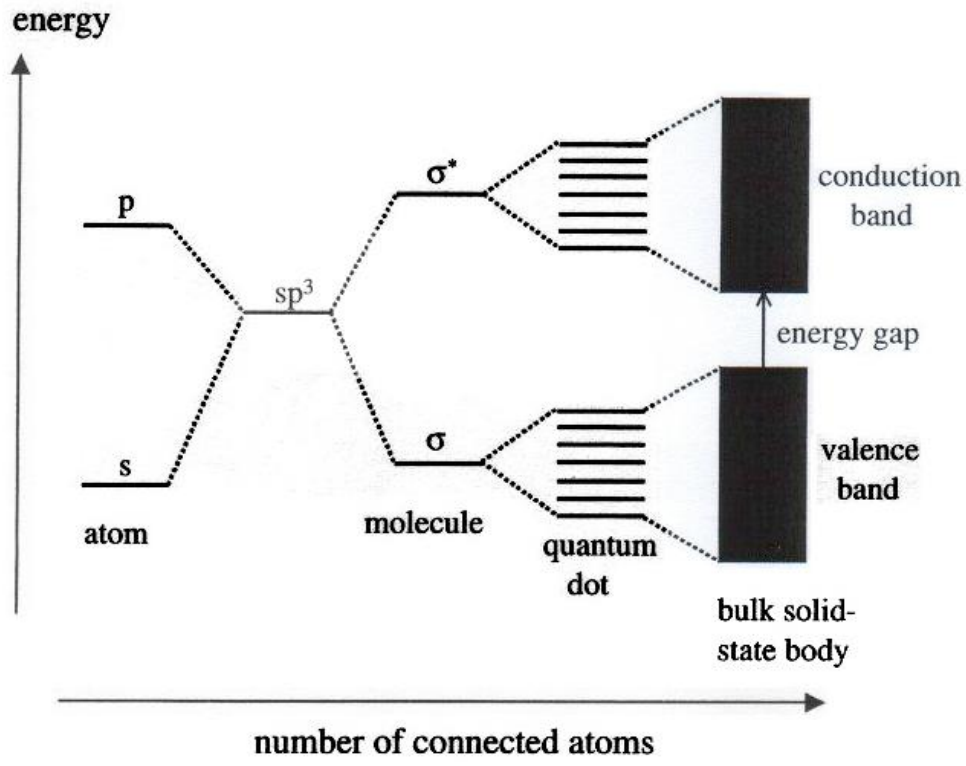

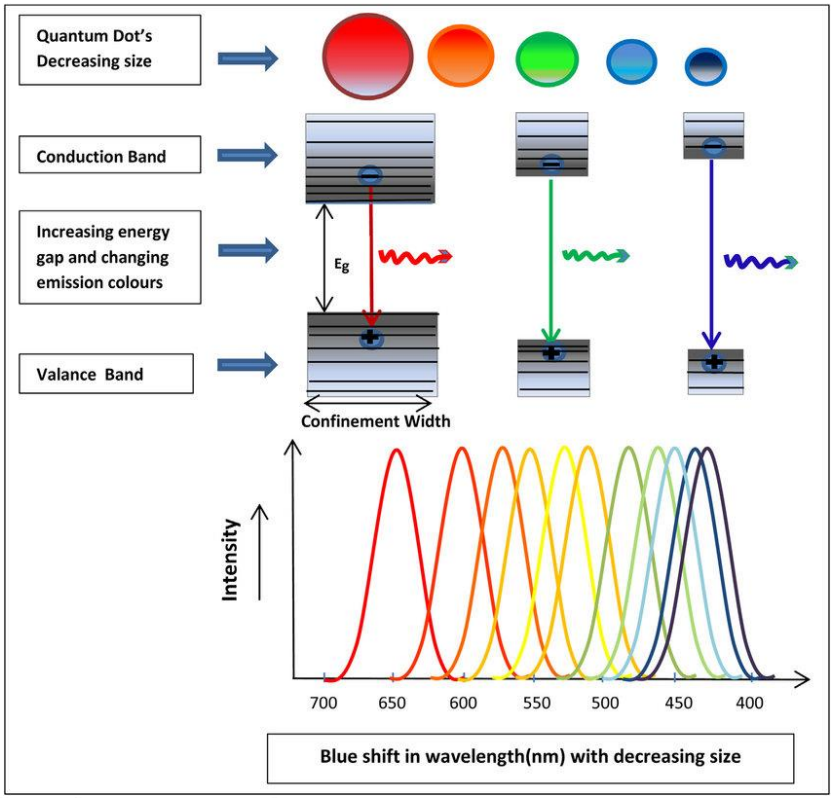

Fig. 2-1 Electronic energy levels depending on the number of bound atoms. By binding more and more atoms together, the discrete energy levels of the atomic orbitals merge into energy bands (here shown for a semiconducting material) [16]. Therefore semiconducting nanocrystals (quantum dots) can be regarded as a hybrid between small molecules and bulk material.

Properties of Metal Nanoparticles

size range	class	major property	example
< 2 nm	cluster	molecular- to metal-like	Au_{11}, Au_{28}, Au_{39}, Au_{55}, Au_{102}
2 – 10 nm	catalytic particle	enhanced catalytic activity	tiny nanoparticles
0–300 nm	plasmonic crystal	surface plasmon resonance	polyhedrons, rods, wires, plates

Synthesis of metal nanoparticles

***PVD** (physical vapor deposition)*

formation of clusters in the gas phase - Au metal as strating material

for example, the nanoparticles are formed from bulk metal by irradiating it with a laser beam. At low laser flux, the material is heated by the absorbed laser energy and evaporates or sublimates and deposited over a solid support, under UHV condition.

es. cathodic arc deposition, sputter deposition, electron beam physical vapor deposition, laser ablation

***CVD** (chemical vapor deposition)*

organometallic compounds as starting material

In a typical CVD process, the wafer (substrate) is exposed to one or more volatile precursors, which react and/or decompose on the substrate surface to produce the desired deposit. Frequently, volatile by-products are also produced, which are removed by gas flow through the reaction chamber.

Laser Ablation is the process of removing material from a solid (or occasionally liquid) surface by irradiating it with a laser beam. At low laser flux, the material is heated by the absorbed laser energy and evaporates or sublimates. At high laser flux, the material is typically converted to a plasma. Usually, laser ablation refers to removing material with a pulsed laser, but it is possible to ablate material with a continuous wave laser beam if the laser intensity is high enough.

***critical issues**: control of the NP size and dispersion, (stability under ambient and/or biological conditions)*

Synthesis of metal nanoparticles in liquid phase

- 12-64 nm J. Turkevitch, P. C. Stevenson, J. Hillier, *Disc. Farady Soc.* **1951**, *11*, 55.

Reduction with **sodium citrate** developped by Frens in 1973:
this is the most used method for the preparation of gold colloids.

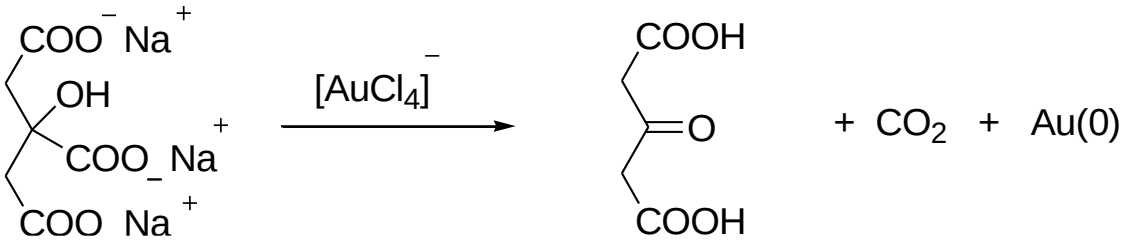

it is easy
- it requires only water
- it requires skills
- has reproducibility issues

NPs size may increases using more diluted solutions.

J. Chem. Edu. 1999, 76, 949.

Synthesis of metal nanoparticles in liquid phase

reduction of $HAuCl_4$ with different reducing agents

- 2-5 nm sodium borohydride ($NaBH_4$)
- 12 nm

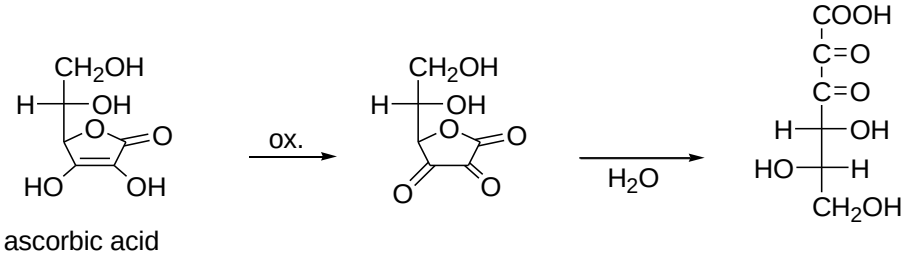

ascorbic acid

- 12-64 nm

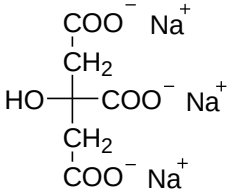

sodium citrate

Synthesis of metal nanoparticles in liquid phase

- the strength of the reducing agent determine the NP size
- the reaction conditions are also very important in determining the average diameter
  - the size may be reduced by: increasing reductant
    decreasing volume
    increasing stirring
    increasing temperature

Synthesis of metal nanoparticles in liquid phase

Electrostatic stabilization: the electrical double layer

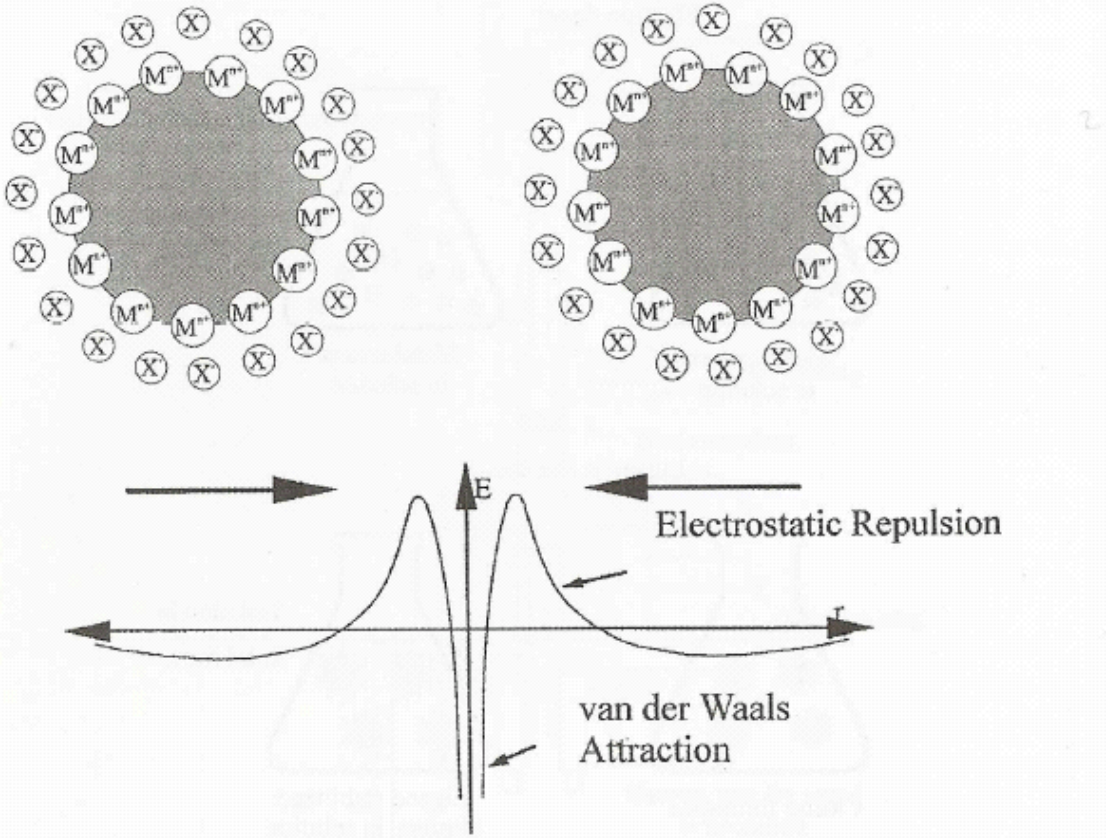

FIGURE 2.24 Electrostatic stabilization of metal colloids. Van der Waals attraction and electrostatic repulsion compete with each other.[27]

the energetic maximum can be easily overtake increasing, for example, the ionic strength or by increasing the thermal movement of the NPs.

Synthesis of metal nanoparticles in liquid phase

Steric stabilization

polymers, surfactants, and ligands may be used to form a protective monolayer

polymers: they should present specific groups that bound to the NPs surface

Gold Number: quantity of polymer that stabilize 1 g of a solution of 50 mg/L of colloidal gold against aggregation in the presence of NaCl 1%

PVP [poly(vinylpyrrolidone)] and **PVA**, poly(vinyl alcohol) o
CTAB (cetyltrimethilammonium bromide)

These polymers have been used also to stabilize Pt and Ag NPs

Characterization of NPs

***TEM** (transmission electron microscopy):* give information about structure Dimension, dispersion, shape, and composition of the metal core

HRTEM high resolution TEM, atomic layers distance.

HAADF-STEM high-angle annular dark-field imaging in the scanning electron microscope

BF-TEM and ADF-STEM tomography (Bright field and annular dark field) electron tomography for 3D reconstruction of nanoparticles shapes.

EDX: energy dispersive X-Ray analysis

X-ray diffraction

XRD

SAXS small-angle X-ray scattering (down to 1 nm)
anomalous SAXS (synchrotron radiation)

WAXS wide-angle X-ray scattering

EDX energy dispersive X-ray spectroscopy

EXAFS extended X-ray absorption fine structure

XPS X-ray photoelectron spectroscopy

Mössbauer spectroscopy

XANES X-ray absorption near-edge structure

***STS** scanning-tunneling spectroscopy*

Characterization of NPs

UV-Vis spectroscopy provides valuable information regarding shape, size, interparticle distance and aggregation of nanoparticles.

DLS, Dynamic light scattering analysis determines the average hydrodynamic size and size distribution profiles of the particles in solution and ζ, zeta potential.

NTA, nanosight traching analysis, NPs populations of different size are recognized

TGA Thermal analysis including thermogravimetric analysis

DSC differential scanning calorimetry: can be used to analyse the amount of organic residues and surface melting properties of the organic coating.

Trasmission Electron Microscope

Jeol 2010F UHR TEM/STEM electron microscope

Trasmission Electron Microscopy

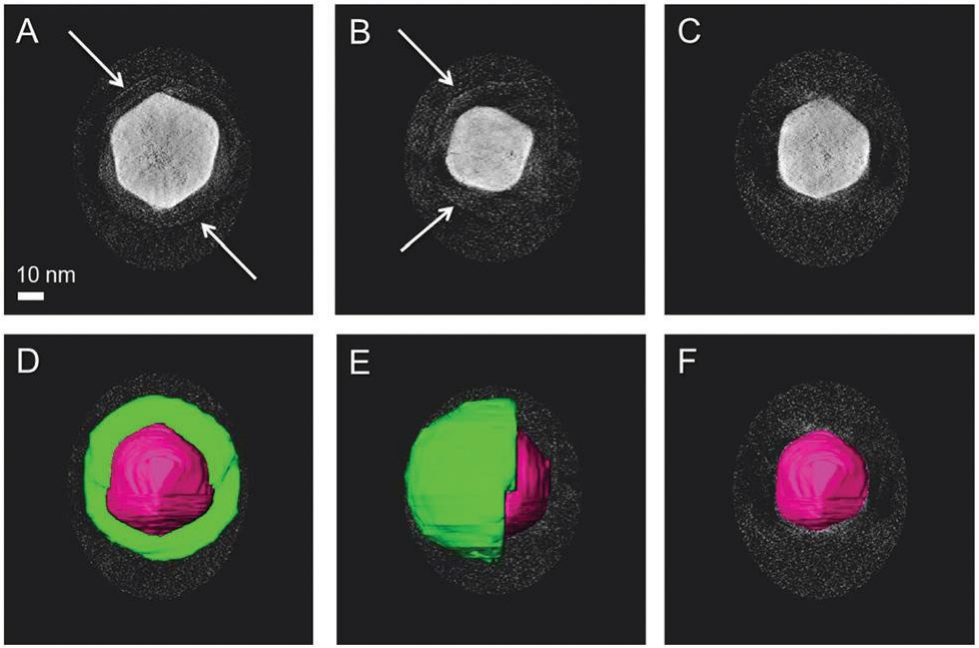

BF-TEM tomography for nanoparticles coated by PEG 1 kDa + PNIPAM 1.2 kDa and stained with $CuSO_4$.
Liz-Marzan L. M. et al. Chem. Commun., 2016, 52, 4278—4281.

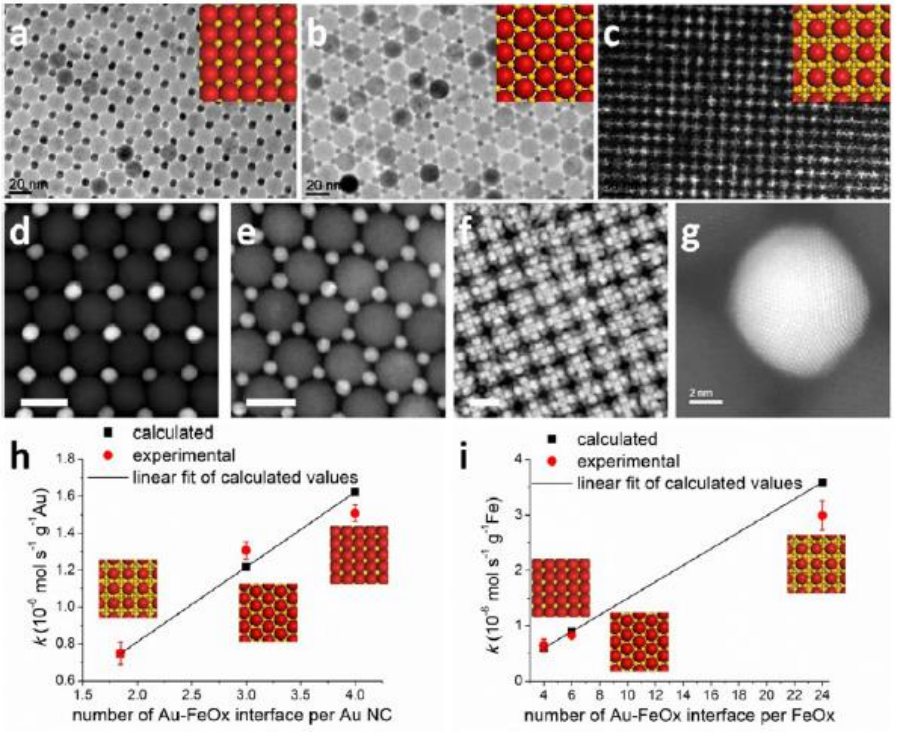

M. Cargnello, P. Fornasiero, C. B. Murray et al.
Science 2013, 341, 771-773.

Trasmission Electron Microscopy

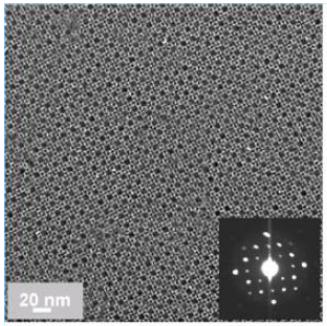

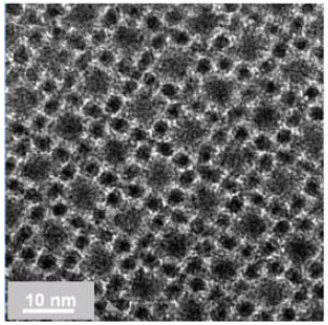

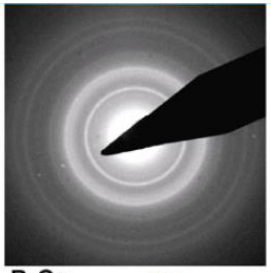

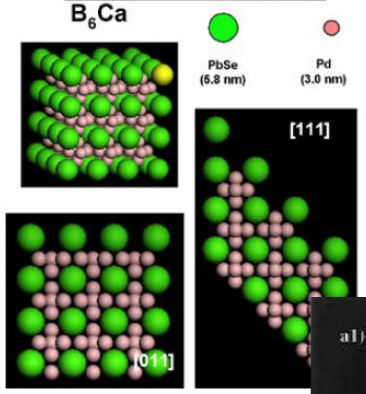

with EDX

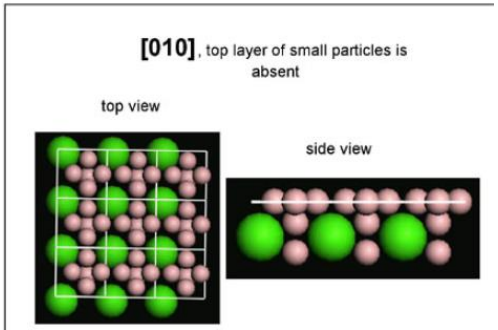

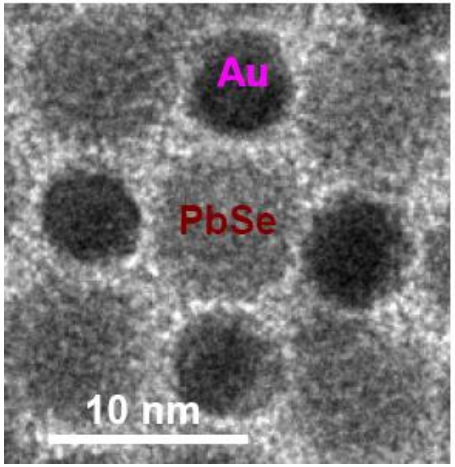

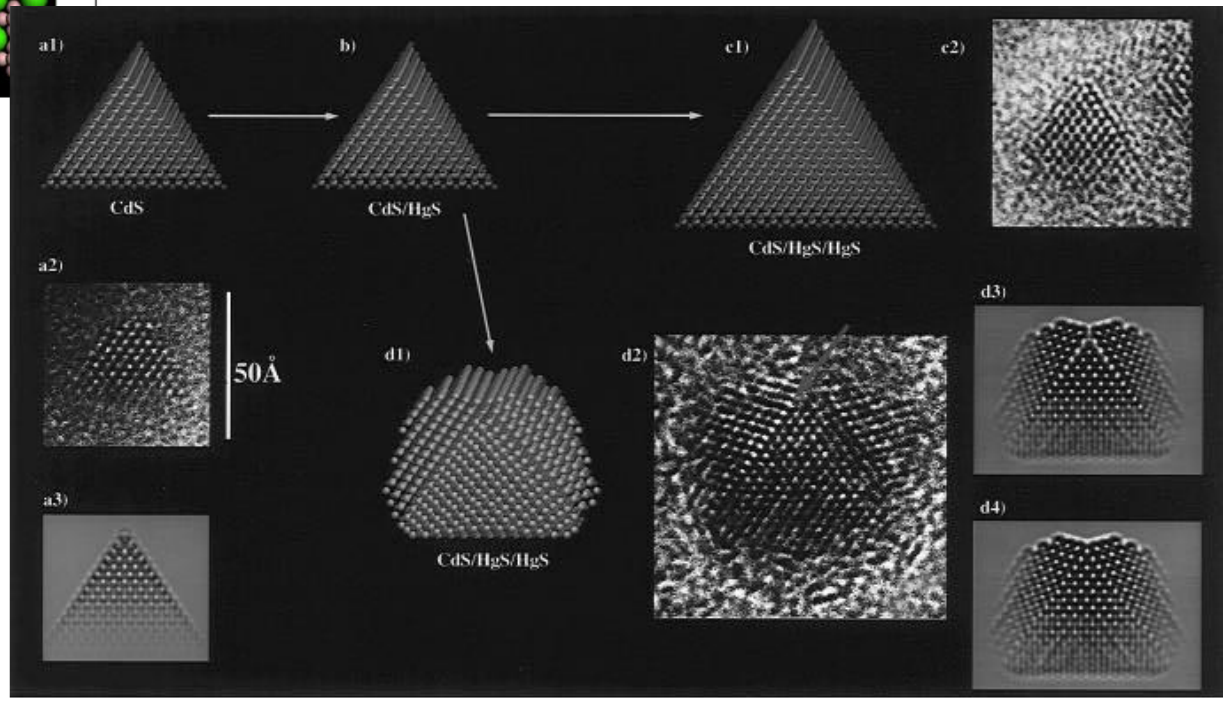

Synthesis of metal nanoparticles in liquid phase

Au, Pd, Pt,

full-shell clusters: clusters are like onions, each atom like to complete his coordination number

for metals the coordination number is 12

the first full-shell cluster is composed of 1+12 = 13 atoms

the shell *n*th includes $10n^2 + 2$ atoms

***n* shell**	1	2	3	4	5	6	7	8	9	10
n. atoms last shell	12	42	92	162	252	362	492	642	812	1002
n. total atoms	13	55	147	309	561	923	1415	2057	2869	3871
% surface atoms	92.3	76.4	62.6	52.4	44.9	39.2	34.8	31.2	28.3	25.8
average d (nm)		1.4	1.9	2.0	2.8	3.0			4.4	4.6

Synthesis of metal nanoparticles in liquid phase

decahedron

only {111} surfaces

icosahedron

for particles < 5 nm

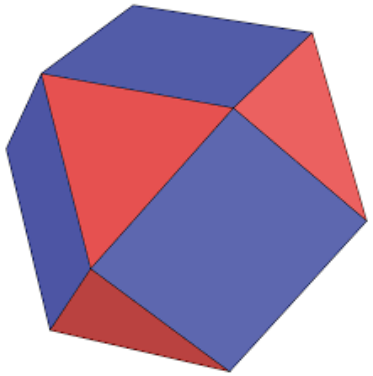

cuboctahedron

for larger particles

UNDECAGOLD

Step 1. $HAuCl_4 + 2PPh_3 + H_2O \xrightarrow{\text{EtOH or THF}} Ph_3PAuCl + Ph_3PO + 3HCl$

Step 2. $Ph_3PAuCl + NaBH_4 \xrightarrow{\text{EtOH or THF}} Au_{11}(PPh_3)_7Cl_3$

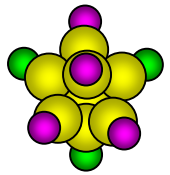

Step 3. $Au_{11}(PPh_3)_7Cl_3 + \sim 30CH_3(CH_2)_{11}SH \xrightarrow{\text{THF}} Au_{11\text{-}13}(PPh_3)_x(SC12)_yCl_z$

Step 4. Column chromatography to remove PPh_3O, Ph_3PAuCl, $[CH_3(CH_2)_{11}S]_2$

"undecagold" derivatives have been widely used as markers of biological compounds and for histochemical analysis

P. A. Bartlett, B. Bauer, S. J. Singer, *J. Am. Chem. Soc.* **1978**, *100*, 5085.
F. Cariati, L. Naldini, *Inorg. Chim. Acta*, **1971**, *5*, 172.

UNDECAGOLD

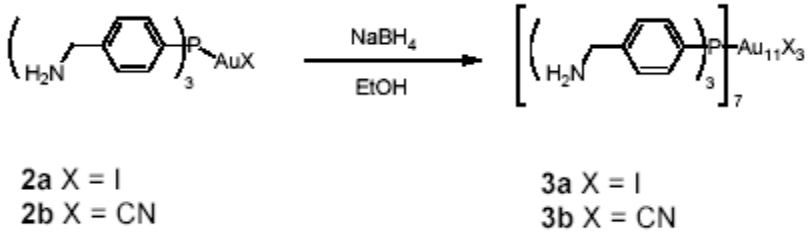

2a X = I
2b X = CN

3a X = I
3b X = CN

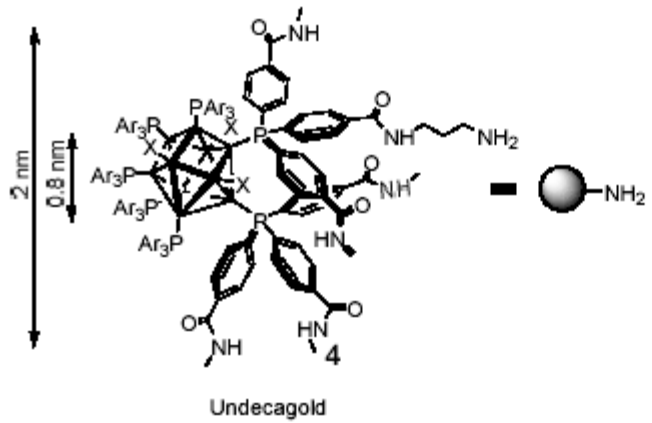

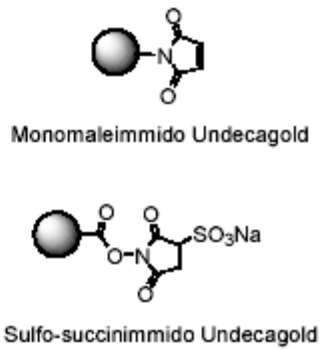

to bound thiols

it reacts with amines

H. Yang, P. A. Frey, *Biochemistry*, **1984**, *23*, 3849, 3857, 3863.

- conjugates of peptide, ATP, nucleic acids, lipids, phospholipidis, carbohydrates, antibodies, etc. have been prepared.

Monolayer protected clusters MPCs

J. CHEM. SOC., CHEM. COMMUN., 1994

Synthesis of Thiol-derivatised Gold Nanoparticles in a Two-phase Liquid–Liquid System

Mathias Brust, Merryl Walker, Donald Bethell, David J. Schiffrin and Robin Whyman

Department of Chemistry, The University of Liverpool, PO Box 147, Liverpool, UK L69 3BX

Using two-phase (water–toluene) reduction of $AuCl_4^-$ by sodium borohydride in the presence of an alkanethiol, solutions of 1–3 nm gold particles bearing a surface coating of thiol have been prepared and characterised; this novel material can be handled as a simple chemical compound.

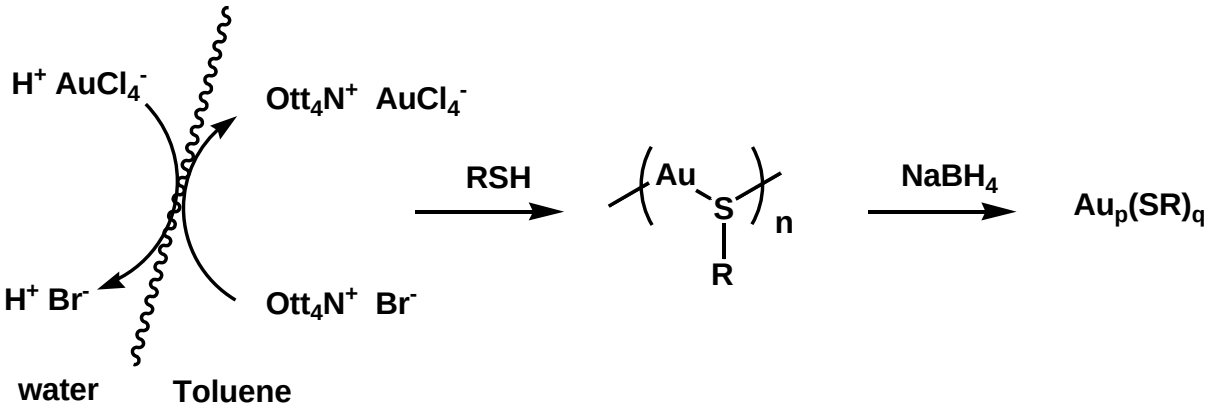

➡ MPCs OF DIFFERENT SIZE MAY BE OBTAINED USING DIFFEREN REACTION CONDITIONS:

■ RATIO RSH/Au ■ REDUCTION RATE ■ TEMPERATURE

Au NPs synthesis

Revised View of the Two-Phase Brust-Schiffrin Au Nanoparticle Synthesis

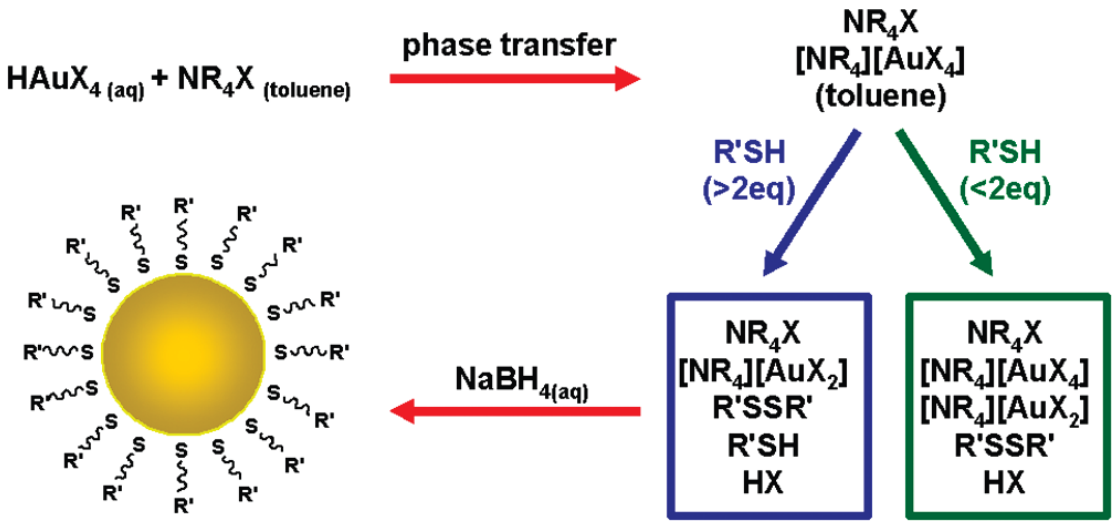

P. J. G. Goulet, R. Bruce Lennox J. Am. Chem. Soc. ***2010****, 132, 9582–9584.*

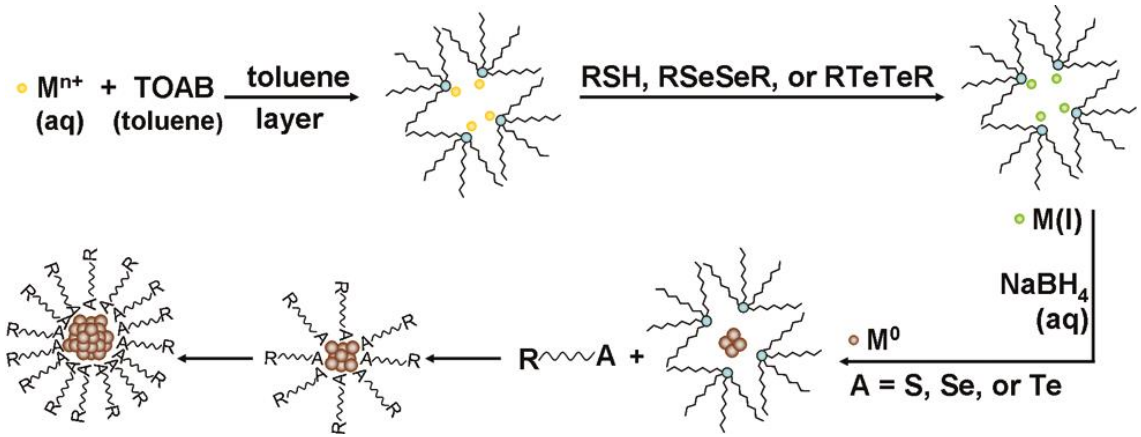

Y. Li, O. Zaluzhna, B. Xu, Y. Gao, J. M. Modest, Y. J. Tong J. Am. Chem. Soc. ***2011****, 133, 2092–2095.*

Nanoparticles – Au_{140}

the core

Au_{140}

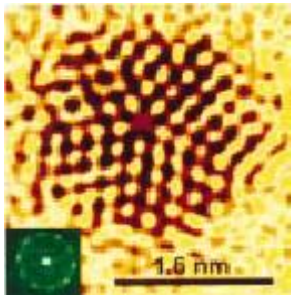

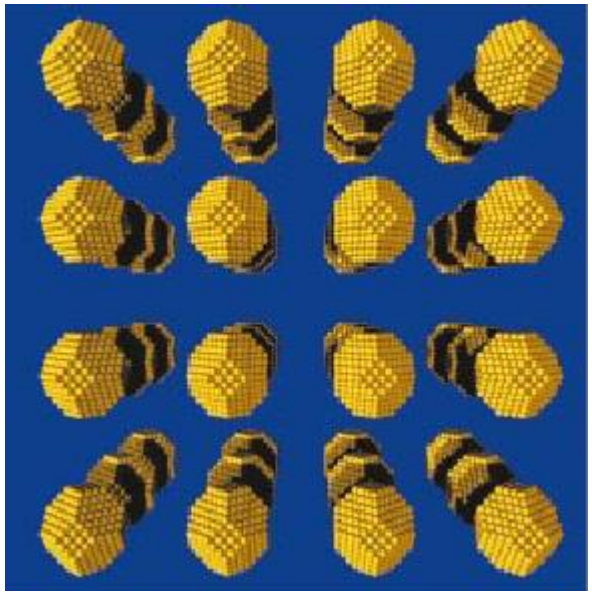

Whetten, R. L. et al. *Acc. Chem. Res.* **1999**, *32*, 397

Nanoparticles – the core

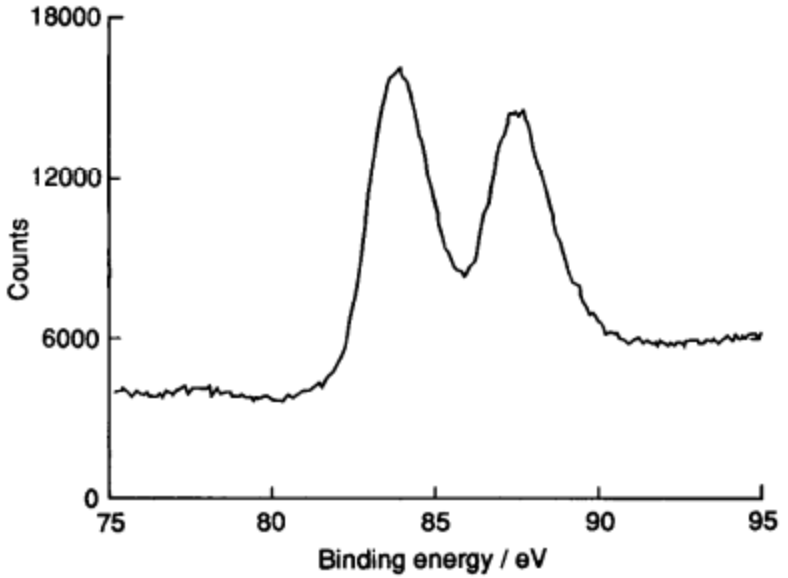

Fig. 3 XPS spectrum of the nanoparticles showing the Au $4f_{7/2}$ and $4f_{5/2}$ doublet with binding energies of 83.8 and 87.5 eV respectively. These are typical values for Au^0.

XPS - **X-ray photoelectron spectroscopy** is a surface-sensitive quantitative spectroscopic technique that measures the elemental composition at the parts per thousand range, empirical formula, chemical state and electronic state of the elements that exist within a material. XPS spectra are obtained by irradiating a material with a beam of X-rays while simultaneously measuring the kinetic energy and number of electrons that escape from the top 0 to 10 nm of the material being analyzed.

Nanoparticles - the monolayer

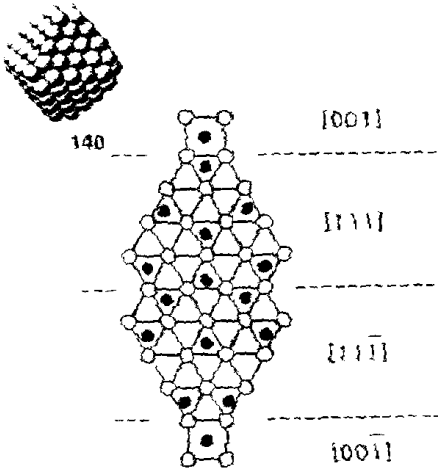

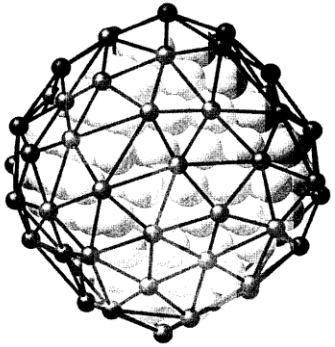

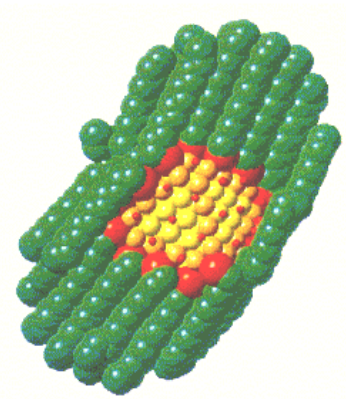

200 K

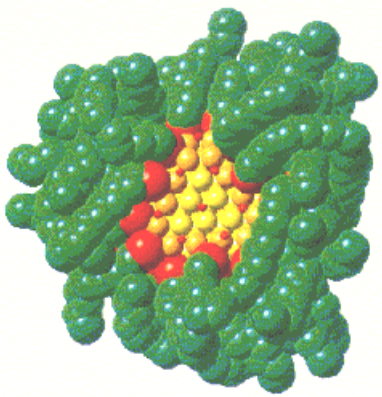

350 K

$Au_{140}(C_{12}H_{25}S)_{62}$

W. D. Luedtke, U. Landman *J. Phys. Chem.* **1996**, *100*, 13323; *J. Phys. Chem. B* **1998**, *102*, 6566

Au-NPs

Structure of a Thiol Monolayer–Protected Gold Nanoparticle at 1.1 Å Resolution

Science **2007**, *318*, 430.

Pablo D. Jadzinsky,[1,2]* Guillermo Calero,[1]* Christopher J. Ackerson,[1]†
David A. Bushnell,[1] Roger D. Kornberg[1]‡

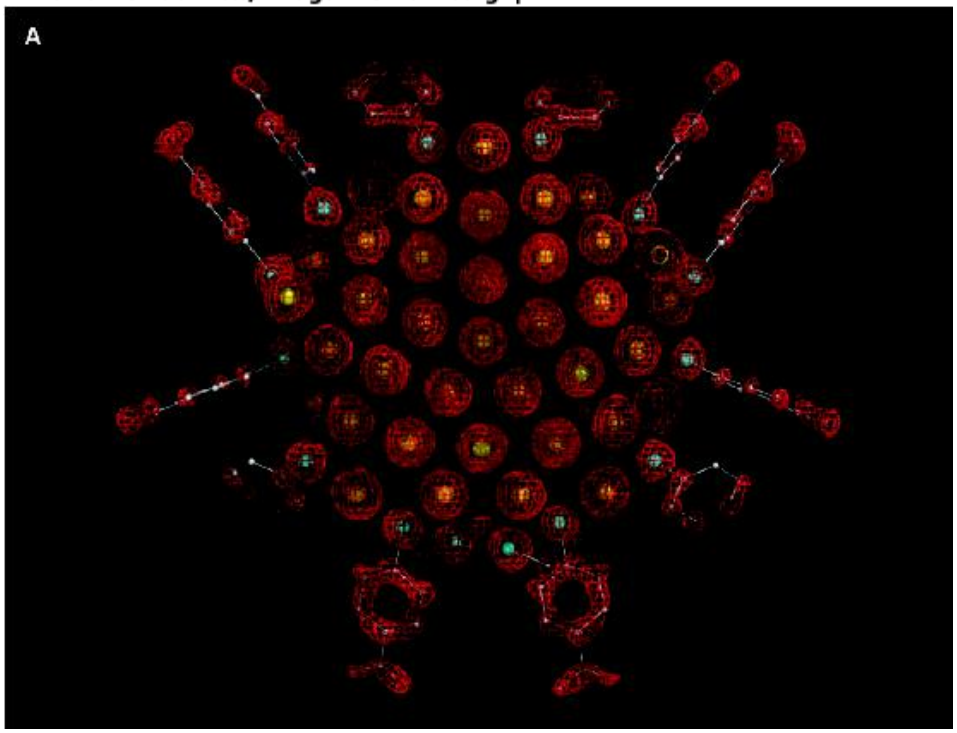

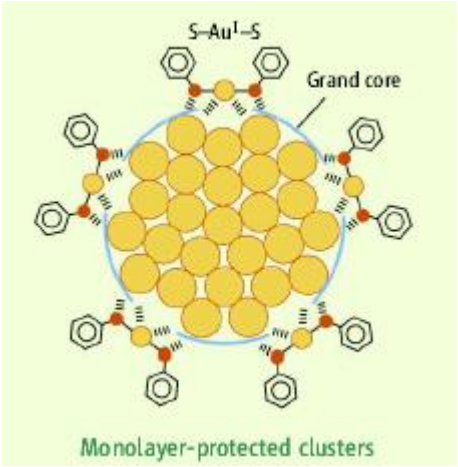

Fig. 1. X-ray crystal structure determination of the Au_{102}(p-MBA)$_{44}$ nanoparticle. (A) Electron density Map (redmesh) and atomic structure (gold atoms depicted as yellow spheres, and p-MBA shown as framework and with small spheres [sulfur in cyan, carbon in gray, and oxygen in red]).

Structure of a thiol monolayer-protected Gold Nanoparticle at 1.1 Å resolution

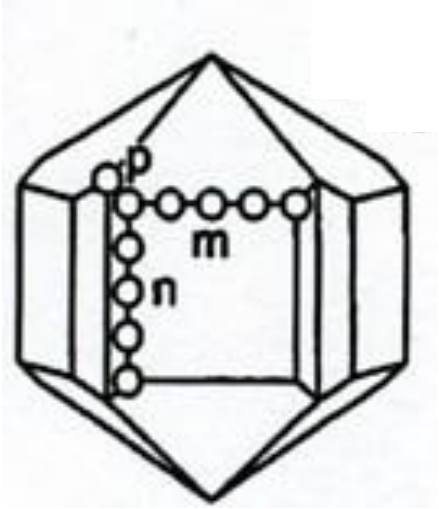

MD (m,n,p)

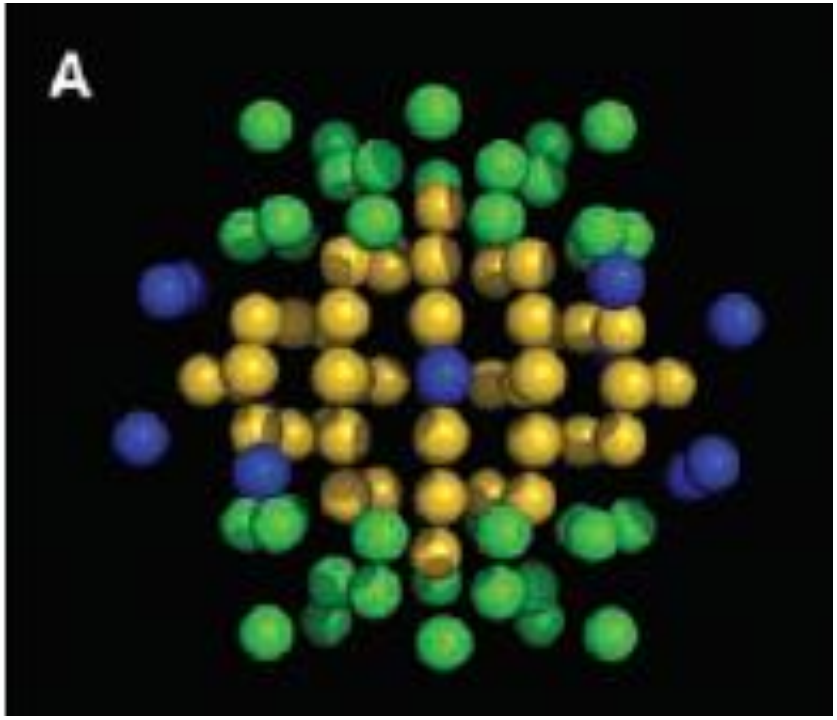

Fig.A: Packing of gold atoms in the nanoparticle. (A) MD (2,1,2) in yellow, two 20-atom“caps” at the poles in green, and the 13-atom equatorial band in blue.

Structure of a thiol monolayer-protected Gold Nanoparticle at 1.1 Å resolution

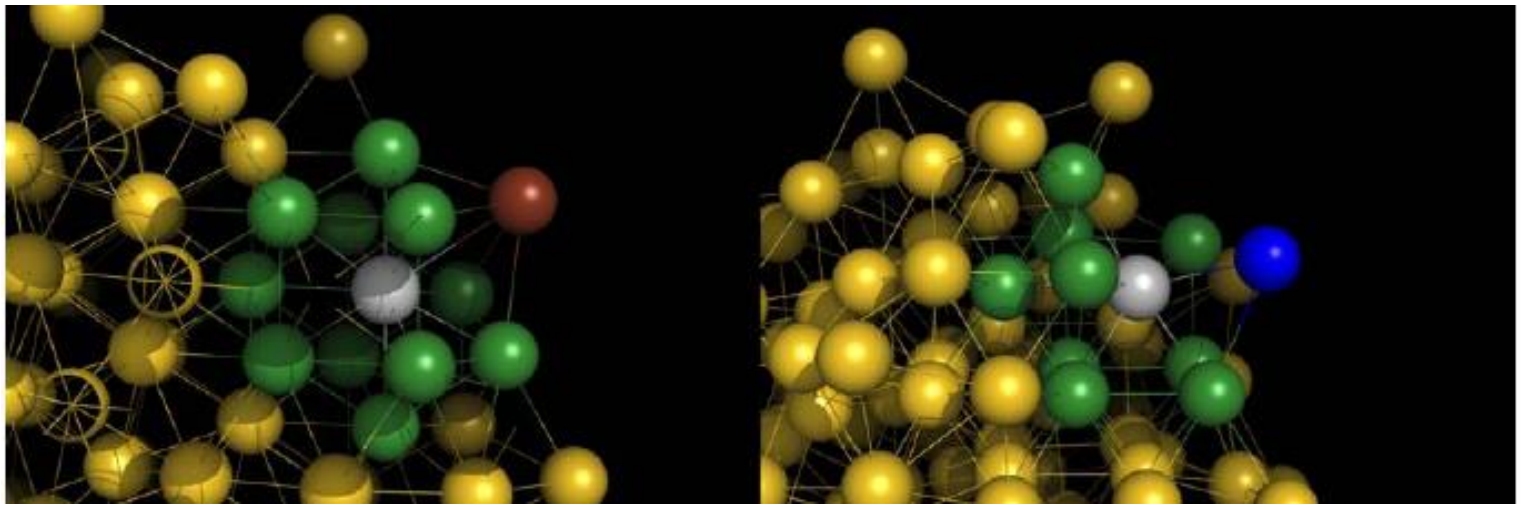

The local environments of the 13 atoms of the equatorial band.

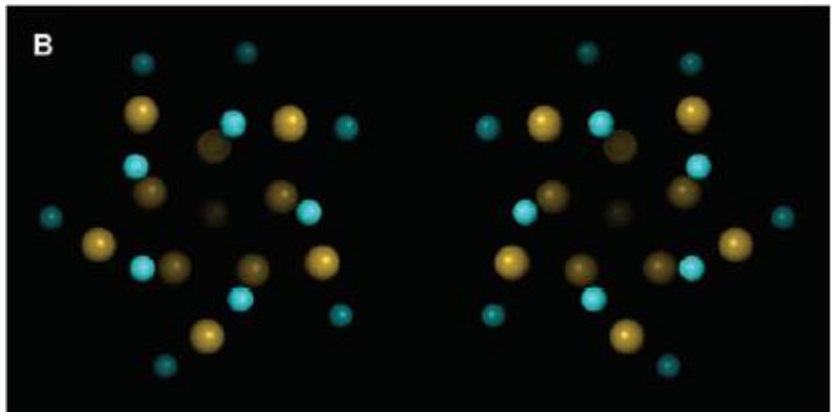

View down the cluster axis of the two enantiomeric particles

Structure of a thiol monolayer-protected Gold Nanoparticle at 1.1 Å resolution

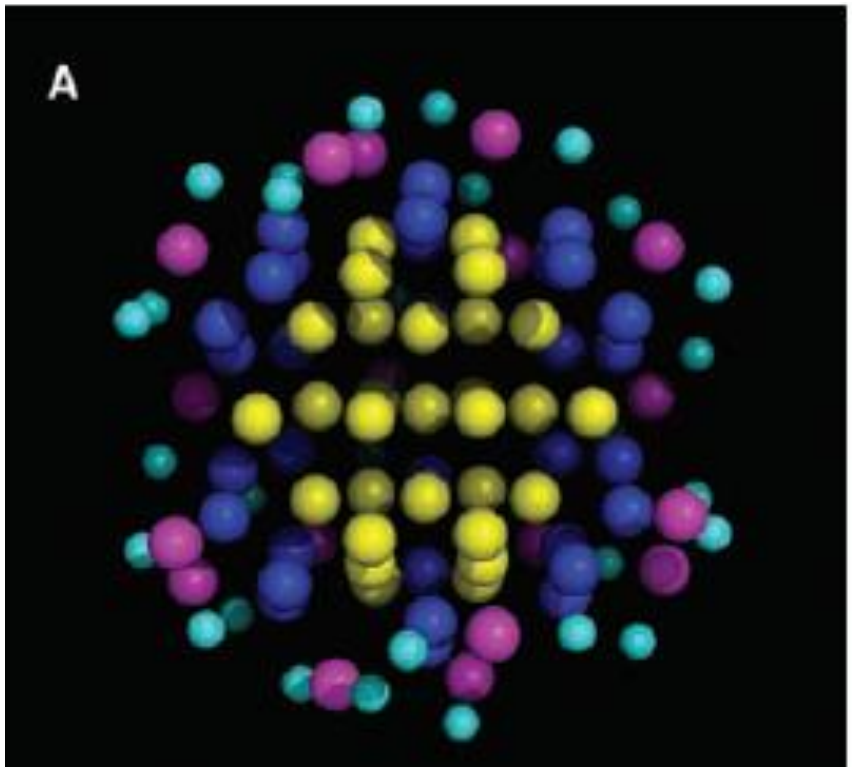

Successive shells of gold atoms interacting with zero (yellow), one (blue), or two (magenta) sulfur atoms. Sulfur atoms are cyan.

Histogram of distances from the center of the cluster of the different shells. Yellow, the 49-atom MD; brown, gold atoms bound to one sulfur atom; blue, gold atoms bound to two sulfur atoms; cyan, sulfur atoms.

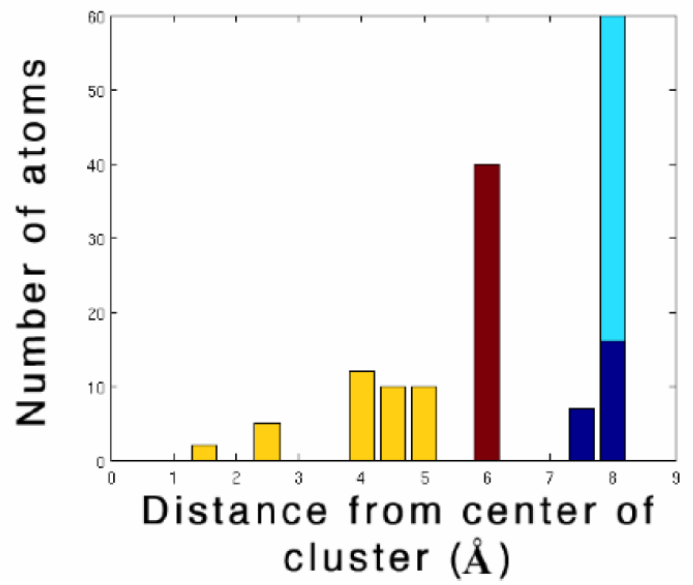

Structure of a thiol monolayer-protected Gold Nanoparticle at 1.1 Å resolution

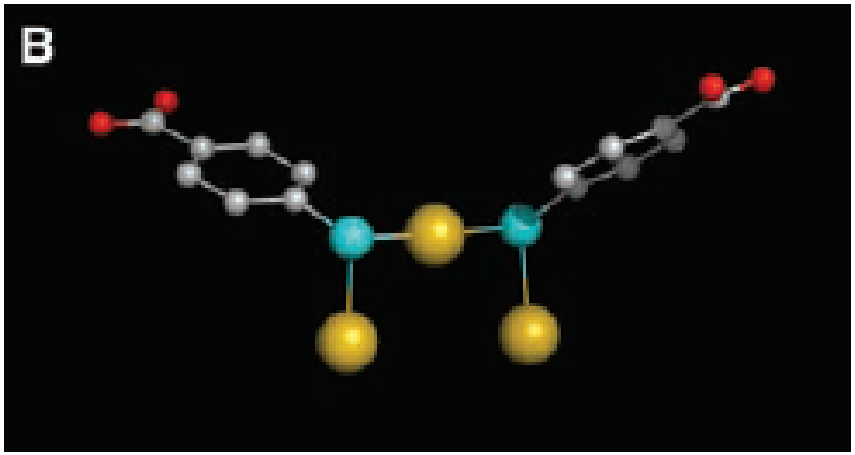

Example of two p-MBAs interacting with three gold atoms in a bridge conformation, here termed a staple motif. Gold atoms are yellow, sulfur atoms are cyan, oxygen atoms are red, and carbon atoms are gray.

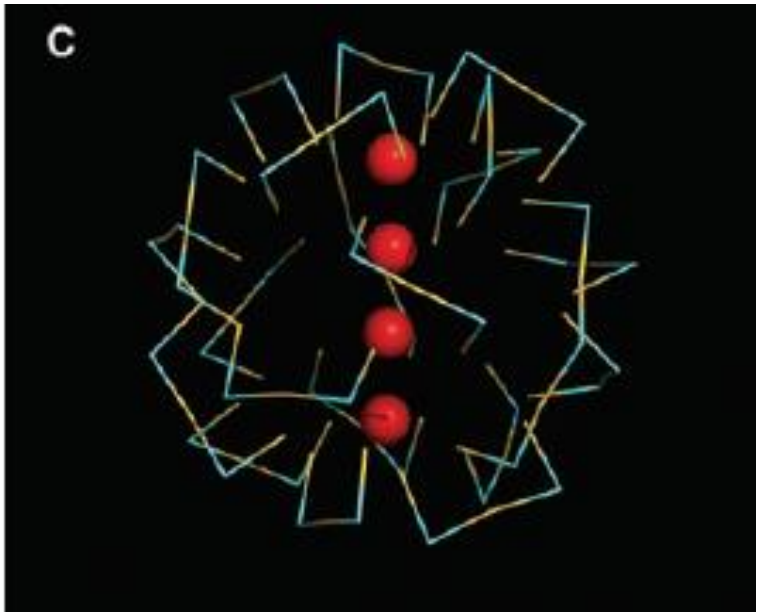

Distribution of staple motifs in the surface of the nanoparticle. Staple motifs are depicted symbolically, with gold in yellow and sulfur in cyan. Only the gold atoms on the axis of the MD are shown (in red).

Structure of a thiol monolayer-protected Gold Nanoparticle at 1.1 Å resolution

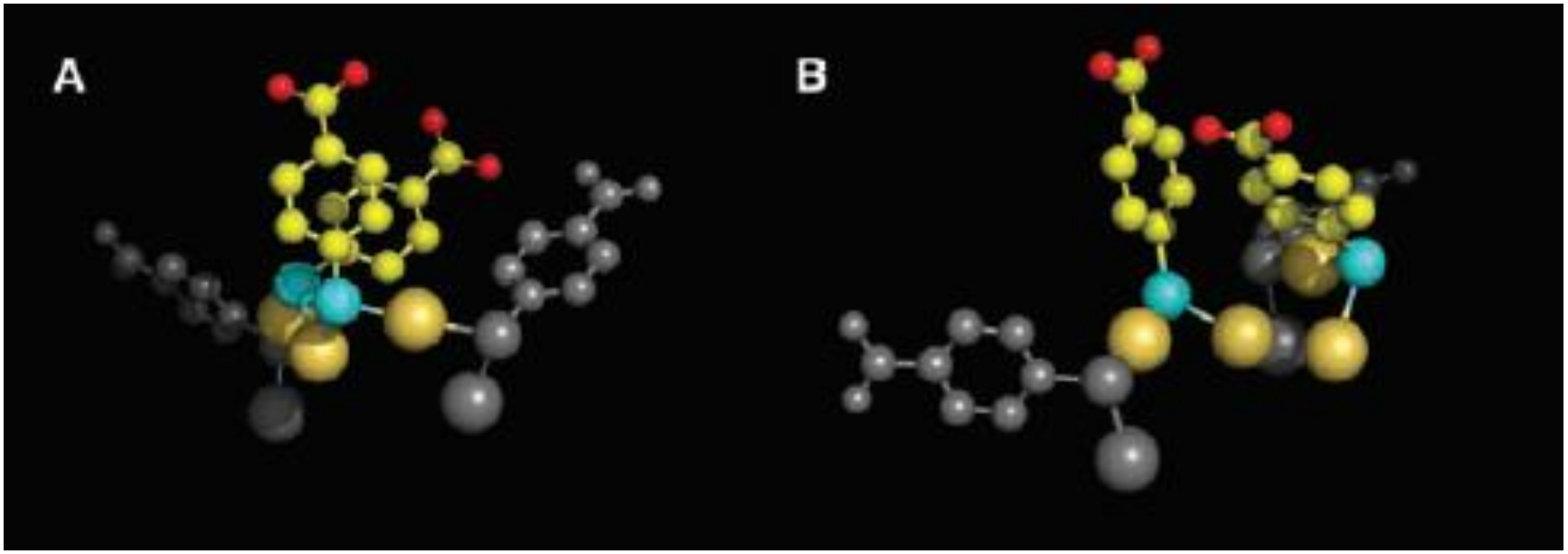

π-π stacking interaction: A) face-to-face B) edge-to-face

Structure of a thiol monolayer-protected Gold Nanoparticle at 1.1 Å resolution

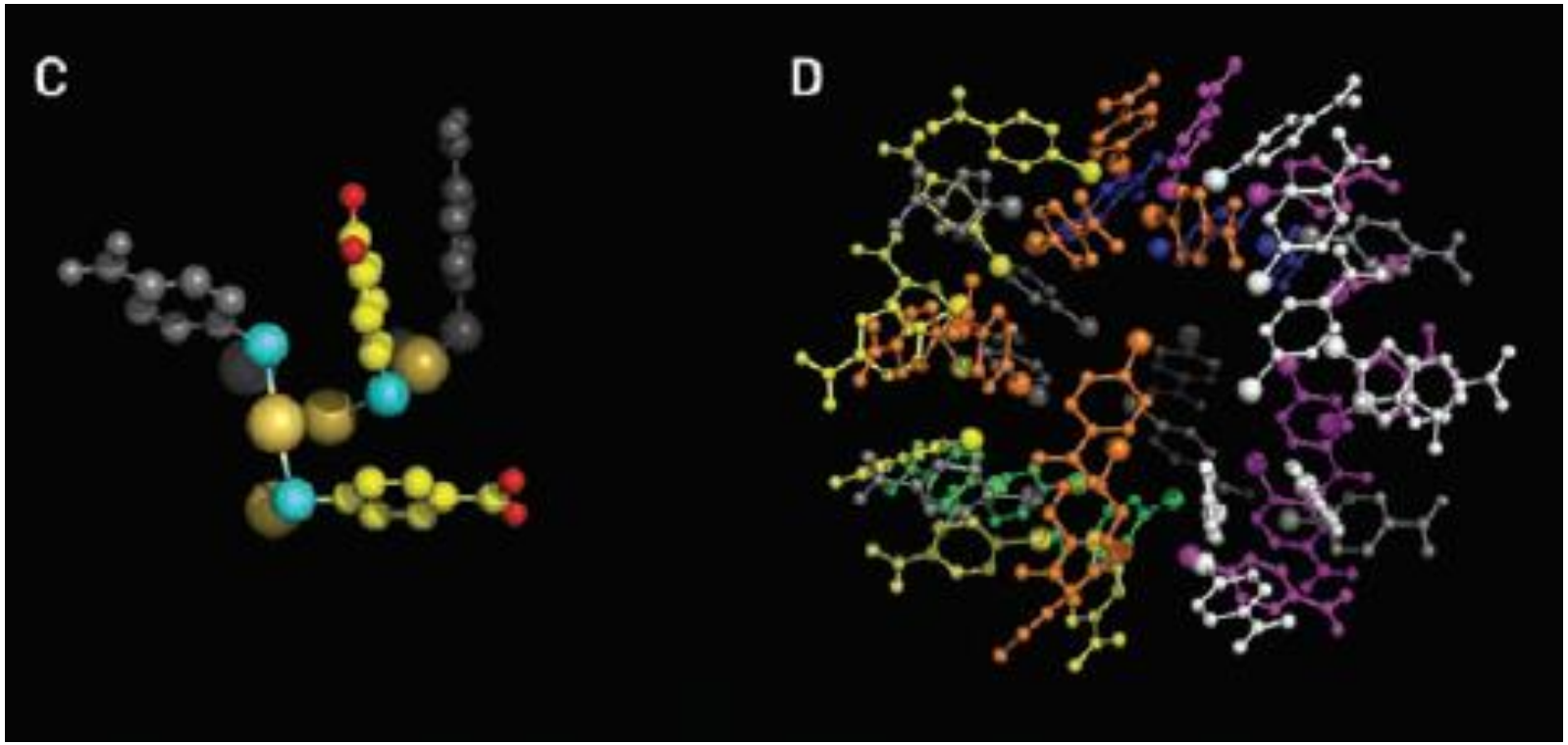

(C) S-Ph stabilization

(D) Chains of interacting p-MBAs, extending across the surface of the nanoparticle, indicated by a different color for each chain.

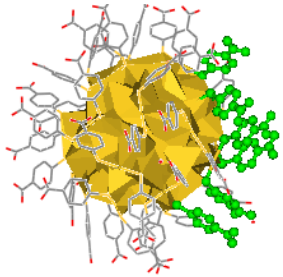

Structure of a thiol monolayer-protected Gold Nanoparticle at 1.1 Å resolution

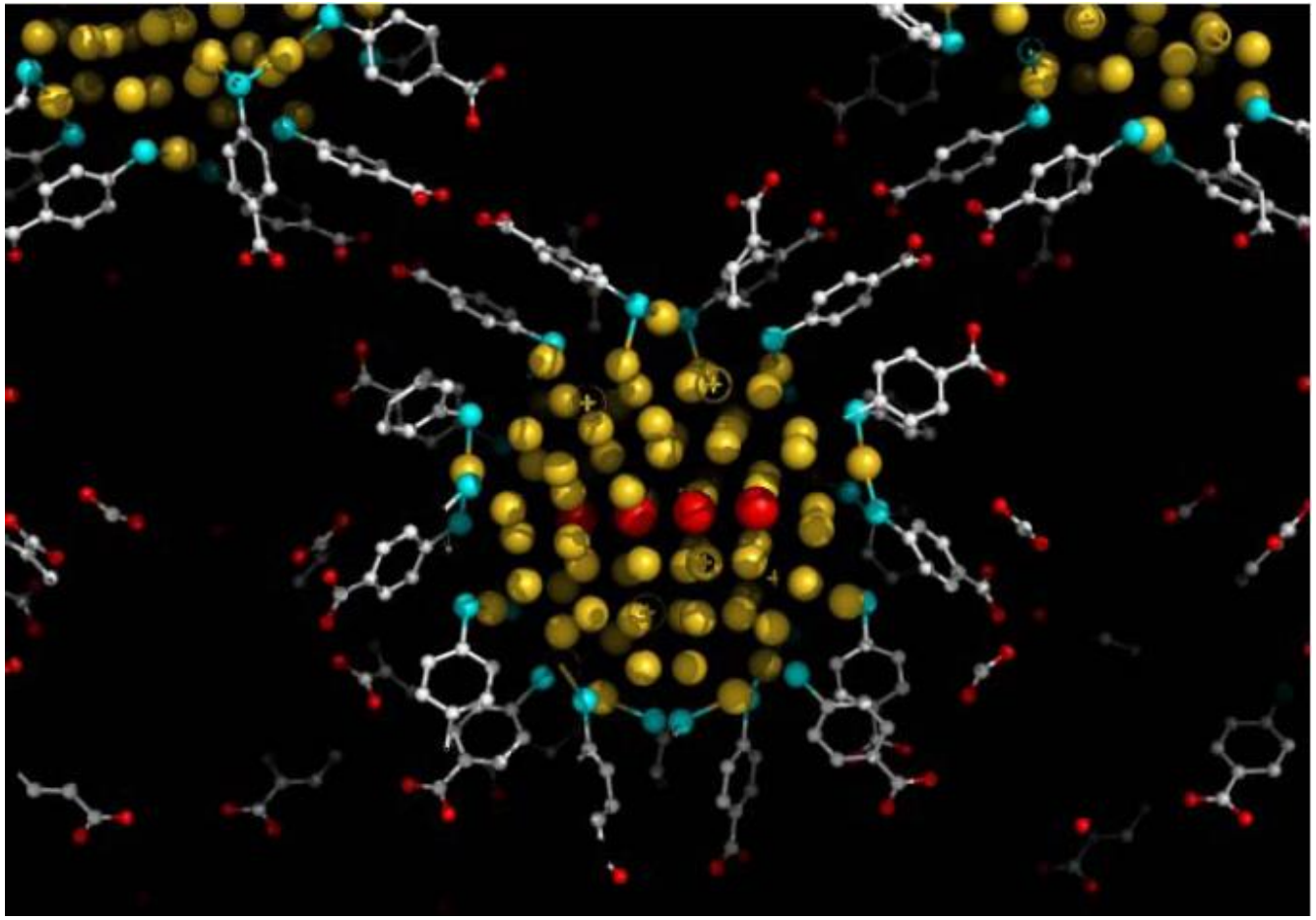

View of the crystal structure showing interparticle interaction mediated throughhydrogen bonding between carboxylic acids.

Structure of a thiol monolayer-protected Gold Nanoparticle at 1.1 Å resolution

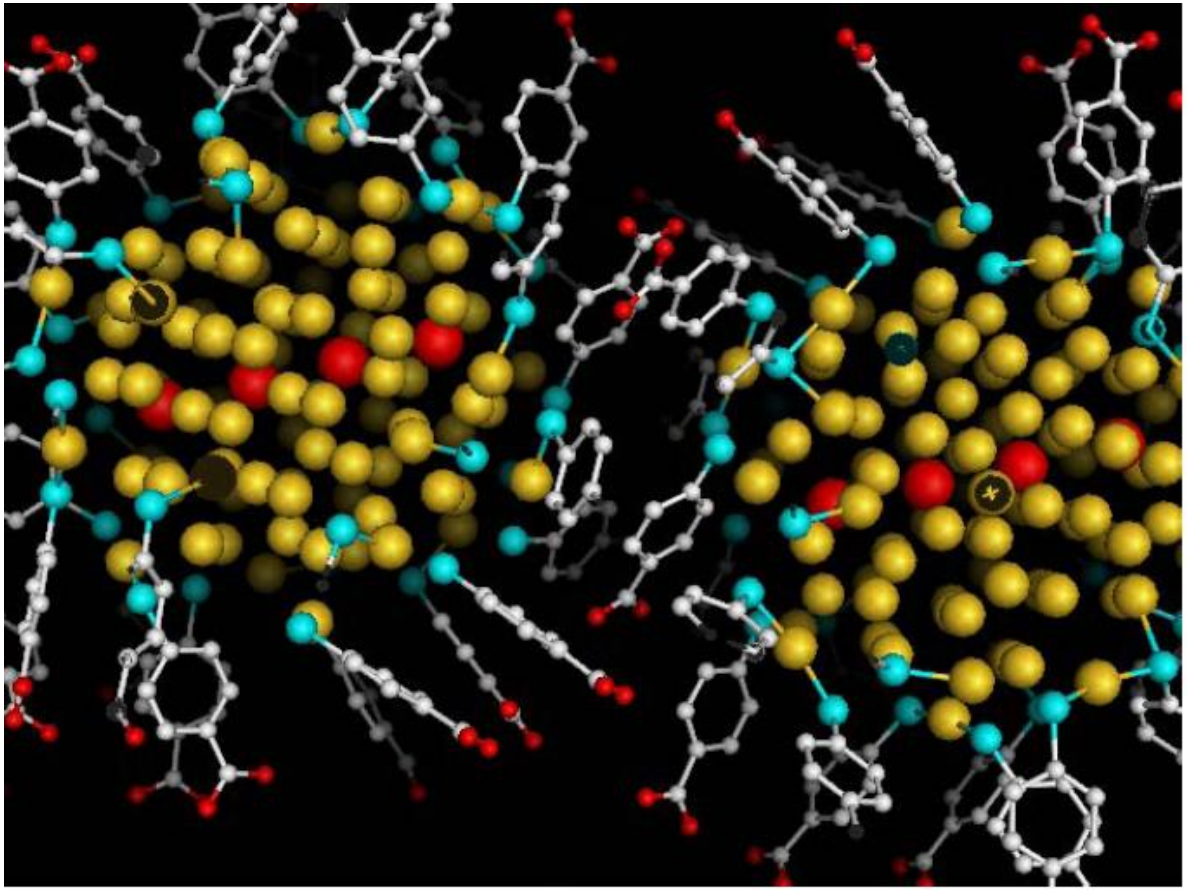

View of the crystal structure showing interparticle interactions mediated between stacked phenyl rings.

Crystal Structure of the Gold cluster [N(C8H17)4][Au25(SCH2CH2Ph)18]

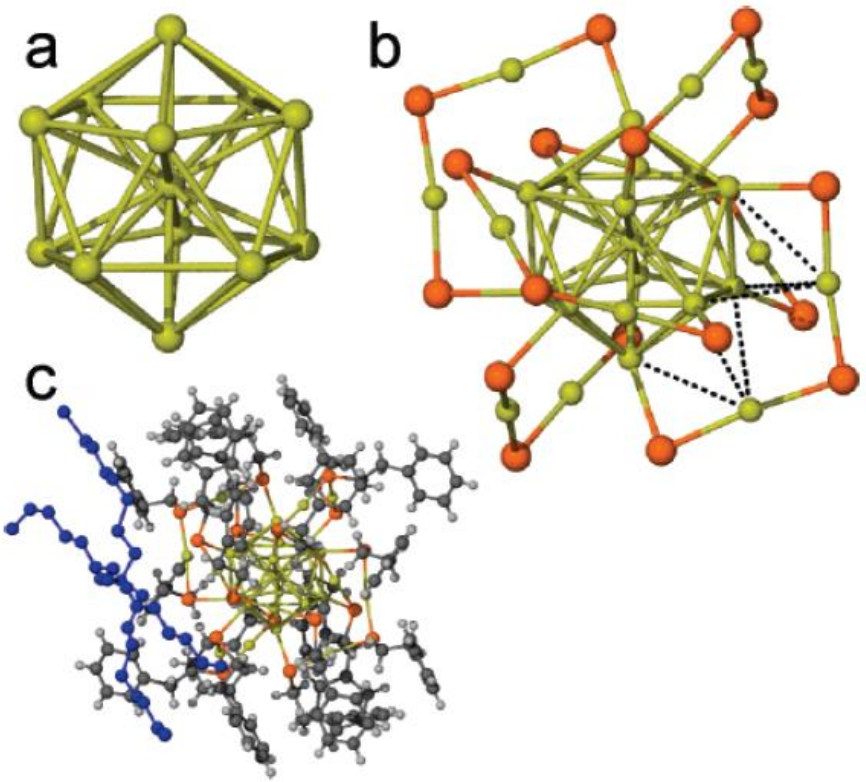

Figure 1. Breakdown of X-ray crystal structure of $[TOA^+][Au_{25}(SCH_2CH_2Ph)_{18}^-]$ as seen from [001]. (a) Arrangement of the Au_{13} core with 12 atoms on the vertices of an icosahedron and one in the center. (b) Depiction of gold and sulfur atoms, showing six orthogonal $-Au_2(SCH_2CH_2Ph)_3-$ "staples" surrounding the Au_{13} core (two examples of possible aurophilic bonding shown as dashed lines). (c) $[TOA^+][Au_{25}(SCH_2CH_2Ph)_{18}^-]$ structure with the ligands and TOA^+ cation (depicted in blue) (Legend: Gold = yellow; Sulfur = orange; Carbon = gray; Hydrogen = off-white; the TOA^+ counterion is over two positions with one removed for clarity).

M. W. Heaven, A. Dass, P. S. White, K. M. Holt, R. W. Murray **J. AM. CHEM. SOC. 2008**, 130, 3754-3755

Nanoparticles - spontaneous ordering

Au NPs of 4.5 ± 0.8 and 7.8 ± 0.9 nm

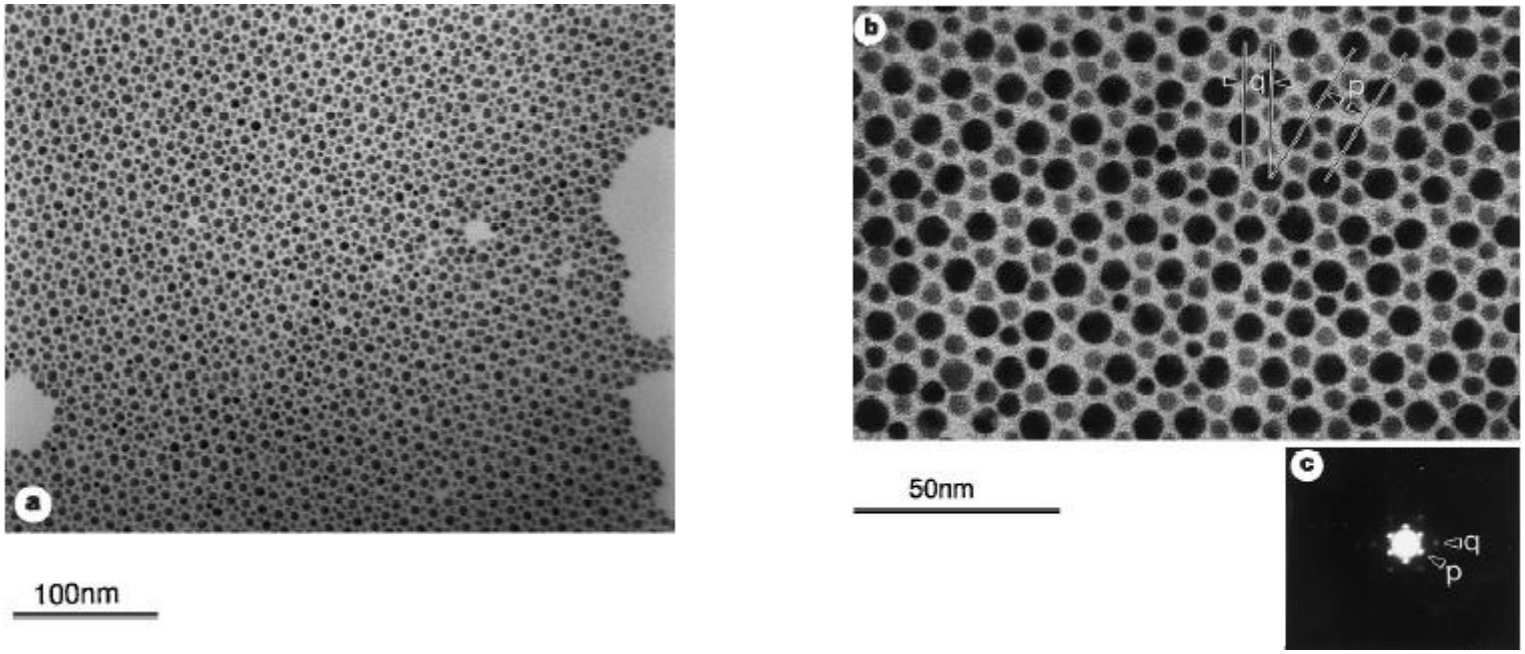

An ordered raft comprising Au nanoparticles of two distinct sizes with R_B/R_A < 0:58. Shown are electron micrographs at low (a) and higher (b) magnification. c, The low-angle superlattice electron diffraction pattern obtained from this bimodal raft structure.

C. J. Kiely, J. Fink,M. Brust, D. Bethell, D. J. Schiffrin, *Nature*, **1998**, *396*, 444.

3D alkanethiolate monolayers

Scheme 1. A Schematic 2D Representation of the RS/Au Nanoparticle Packing Structure in the Solid State[a]

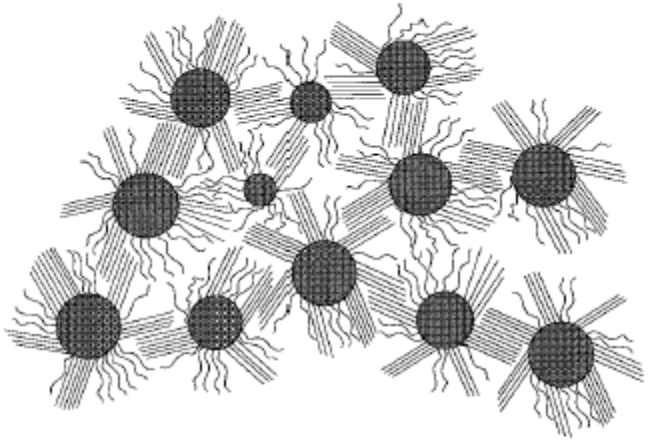

[a] In this description, *domains* or *bundles* of ordered alkylthiolate chains on a given Au particle will interdigitate into the chain domains of neighboring particles in order to compensate for the substantial decrease in the chain density which occurs toward the methyl chain end. Chains with large populations of *gauche* bonds may arise from (i) those which occupy interstitial regions in the particle lattice and cannot efficiently overlap with adjacent chains or from (ii) chains residing at domain boundaries.

Scheme 2. The Types of Chain Dynamic Processes Suggested by the ^{2}H NMR Line Shapes of the Deuterated $C_{18}S$/Au Nanoparticles[a]

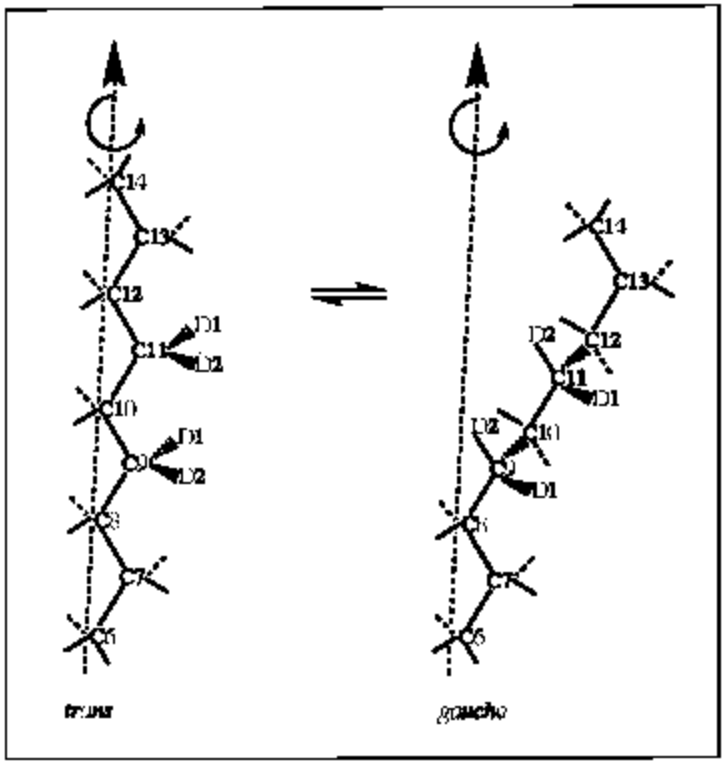

[a] These processes involve *trans-gauche* bond isomerization and pseudorotational motion of individual chain segments about the long axis of the alkanethiolate molecule.

A. Badia, L. Cuccia, L. Demers, F. Morin, B. R. Lennox, *J. Am. Chem. Soc*., **1997**, *119*, 2682.

3D alkanethiolate monolayers

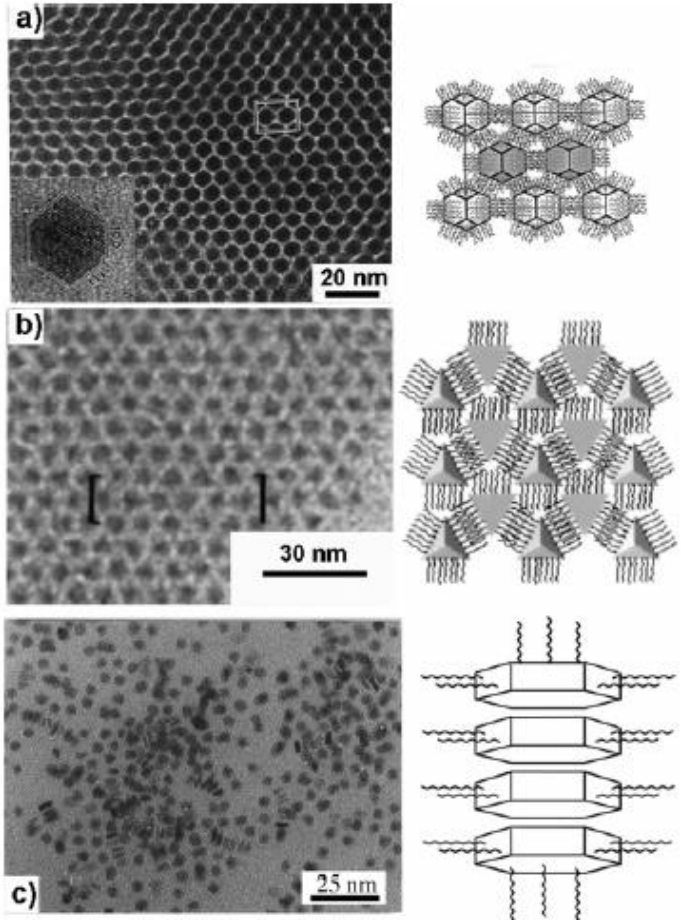

Figure 11. (a) (Left) TEM image of a face-centered, cubic packed, array of silver nanoparticles, passivated with a dodecanethiolate monolayer, with a truncated octahedral morphology (see inset). (Right) Representation of the proposed packing of the particles via interdigitation of the bundled alkyl chains on each face. (b) (Left) TEM image of a monolayer of self-assembled silver tetrahedra passivated with dodecanethiolates. The bracketed area most closely matches the proposed model.

Langmuir **1998**, *14*, 17−30

Alkanethiolate Gold Cluster Molecules with Core Diameters from 1.5 to 5.2 nm: Core and Monolayer Properties as a Function of Core Size

Michael J. Hostetler,[†] Julia E. Wingate,[†] Chuan-Jian Zhong,[‡] Jay E. Harris,[†] Richard W. Vachet,[†] Michael R. Clark,[†] J. David Londono,[§] Stephen J. Green,[†] Jennifer J. Stokes,[†] George D. Wignall,[§] Gary L. Glish,[†] Marc D. Porter,[‡] Neal D. Evans,[∥] and Royce W. Murray*,[†]

Table 1. Size and Composition Results for Different Cluster Preparations

preparation conditions[a]	SAXS[b] R_G, nm, max/min	SAXS[c] R_{POROD}, nm	HRTEM[d] R_{TEM}, nm	TGA[e] % organic	NMR[f] CH_3, ν_{FWHM} Hz
−78°,2X,sd	1.7/0.91	0.76	—	30.7	16
0°,2X,fd	—	—	1.1	28.8	21
0°,2X,md	—	—	—	26.7	22.5
0°,2X,sd	1.7/1.0	0.89	1.1	26.2	25.5
RT,1X,fd	1.7/1.2	1.0	—	25.6	24.5
RT,4X,fd	1.7/1.1	0.94	—	24.9	26
RT,2X,sd	1.6/1.2	0.96	—	24.5	27
RT,2X,fd	—	—	—	23.7	25.5
60°,2X,sd	1.4/1.2	0.98	—	24.1	29
90°,2X,sd	—	—	1.1	23.2	32
RT,1/2X,fd	1.6/1.4	1.2	1.2	19.4	37
RT,1/3X,fd	1.8/1.6	1.4	1.4	16.9	45
RT,1/4X,fd	2.1/2.0	1.7	2.0	12.8	53
RT,1/6X,fd	2.9/2.5	2.2	2.2	9.3	126[g]
RT,1/8X,fd	—	—	—	10.4	124[g]
RT,1/10X,fd	—	—	2.4	6.2	144[g]
RT,1/12X,fd	—	—	2.6	11.9	163[g]

[a] Code for preparation conditions: (*a*,*b*,*c*), where *a* represents the temperature at which the reduction was carried out, *b* represents the RSH:$AuCl_4^-$ molar ratio before reduction, and *c* represents the rate of reductant addition (fd, 10 s; md, 2 m; sd, 15 m). [b] SAXS results for Au core radius determined from Guinier plot. [c] SAXS results from Porod plot. [d] HRTEM results, average Au core size from analysis of histogram of HRTEM images. [e] TGA for thermal loss of alkanethiolate fraction of clusters. [f] Proton NMR linewidths. [g] CH_3 ^1H NMR signal obscured; the CH_2 resonance was used instead for these clusters.

Nanoparticles - characterization

TEM

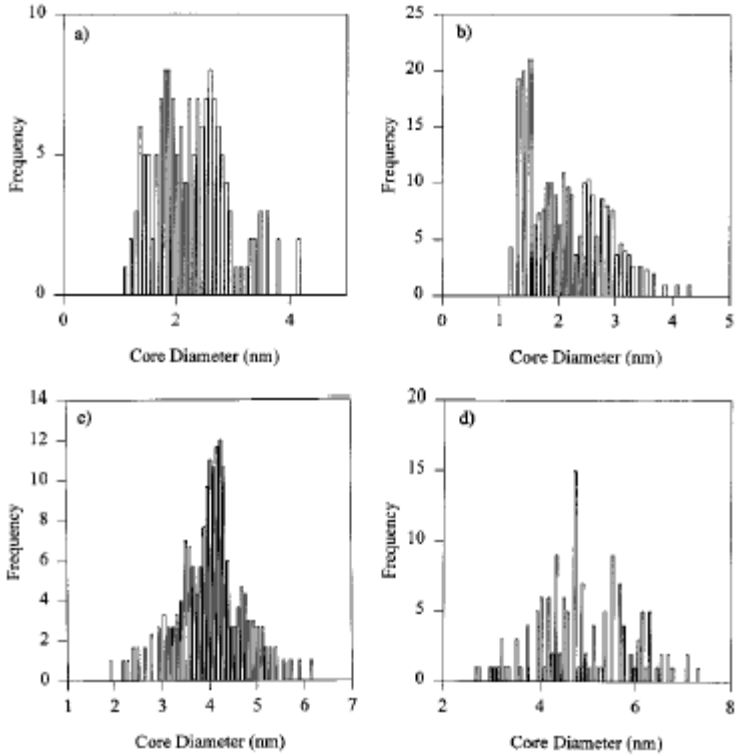

Figure 2. Size histograms (a and d are for films shown in Figure 1): (a) (0°,2X,fd); (b) (0°,2X,sd); (c) (RT,1/4X,fd); (d) (RT, 1/6X,fd).

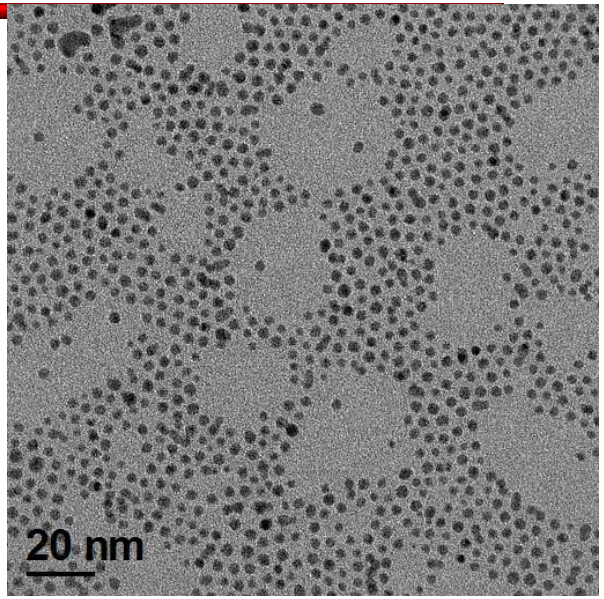

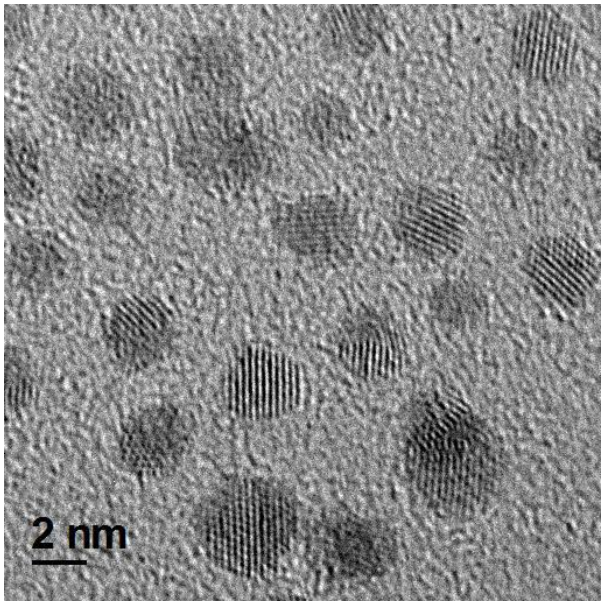

NANOPARTICLES - characterization

Table 2. Results from Modeling of Gold Core Sizes, Shapes, and Alkanethiolate Coverages, and of Size-Dependent T_2 Broadening of Proton NMR of CH_3 Resonances

#atoms (shape)[a]	R_{CORE}, nm	#surface atoms/ %defect/area nm^2	calc TGA %organic/ %coverage/#chains	calc R_{TOTAL}, nm	calc NMR ν_{FWHM}, Hz
79 (TO^+)	0.65	60/60%/8.30	33.0/63%/38	2.6	15
116 (TO^-)	0.71	78/61%/11.36	31.8/68%/53	2.6	16
140 (TO^+)	0.81	96/50%/11.43	27.9/55%/53	2.7	17
201 (TO)	0.87	128/47%/15.22	26.5/55%/71	2.8	18
225 (TO^+)	0.98	140/43%/15.19	24.4/51%/71	2.9	19
309 (CO)	1.1	162/52%/19.64	23.3/57%/92	3.0	22
314 (TO^+)	1.0	174/41%/19.46	22.9/52%/91	3.0	20
459 (TO^+)	1.2	234/36%/24.34	20.2/49%/114	3.1	23
586 (TO)	1.2	272/35%/28.94	19.1/50%/135	3.2	24
807 (TO^+)	1.4	348/31%/34.86	17.1/47%/163	3.3	27
976 (TO^-)	1.5	390/31%/40.02	16.4/48%/187	3.4	28
1289 (TO)	1.6	482/27%/47.22	14.9/46%/221	3.5	32
2406 (TO)	2.0	752/22%/69.86	12.2/43%/326	3.9	42
2951 (TO^+)	2.2	876/21%/79.44	11.4/42%/371	4.1	47; 94[b]
4033 (TO)	2.4	1082/19%/97.00	10.3/42%/453	4.3	55; 110[b]
4794 (TO^+)	2.6	1230/18%/108.28	9.7/41%/506	4.4	61; 122[b]
6266 (TO)	2.8	1472/16%/128.66	8.9/41%/601	4.7	70; 140[b]

[a] CO = cuboctahedron; TO = ideal truncoctahedron (all sides equal); TO^+ = truncoctahedron in which ($0 < n - m \leq 4$), where n is the number of atoms between (111) facets and m is the number of atoms between (111) and (100) facets; TO^- = truncoctahedron in which ($-4 \leq n - m < 0$, $m > 1$). [b] The second value is the calculated linewidth for the methylene peak.

NMR spectroscopy

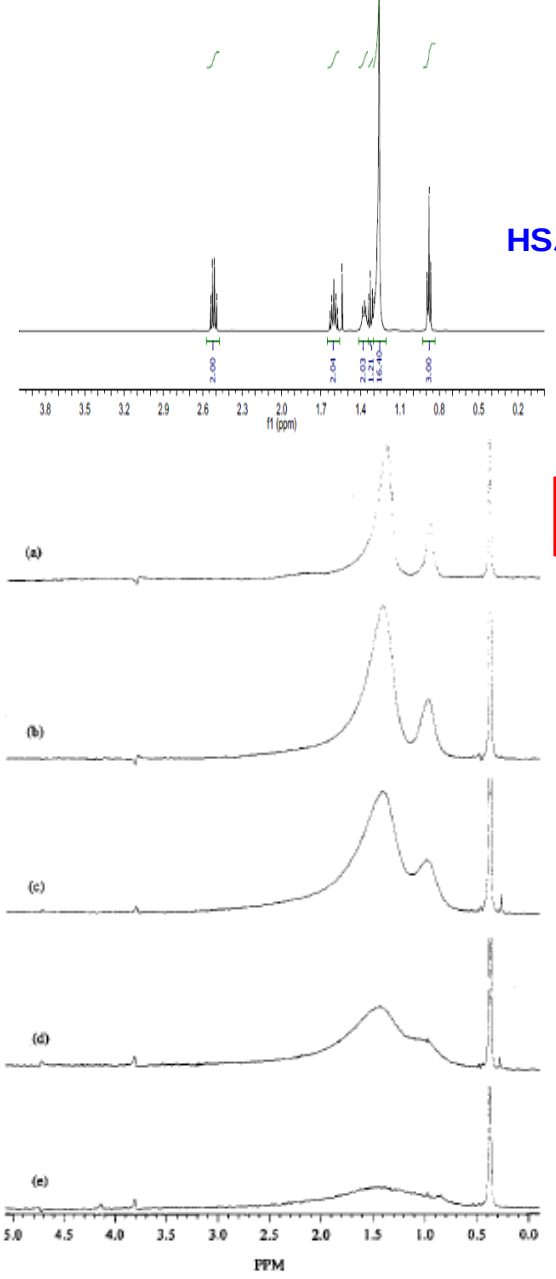

^{1}H

Figure 5. The ^{1}H NMR spectra (C_6D_6) of dodecanethiolate-protected Au clusters. Each spectrum was Fourier transformed using a line broadening of 1 Hz: (a) (−78°,2X,sd); (b) (90°,2X,sd); (c) (RT,1/3X,fd); (d) (RT,1/4X,fd); (e) (RT,1/12X,fd).

^{13}C

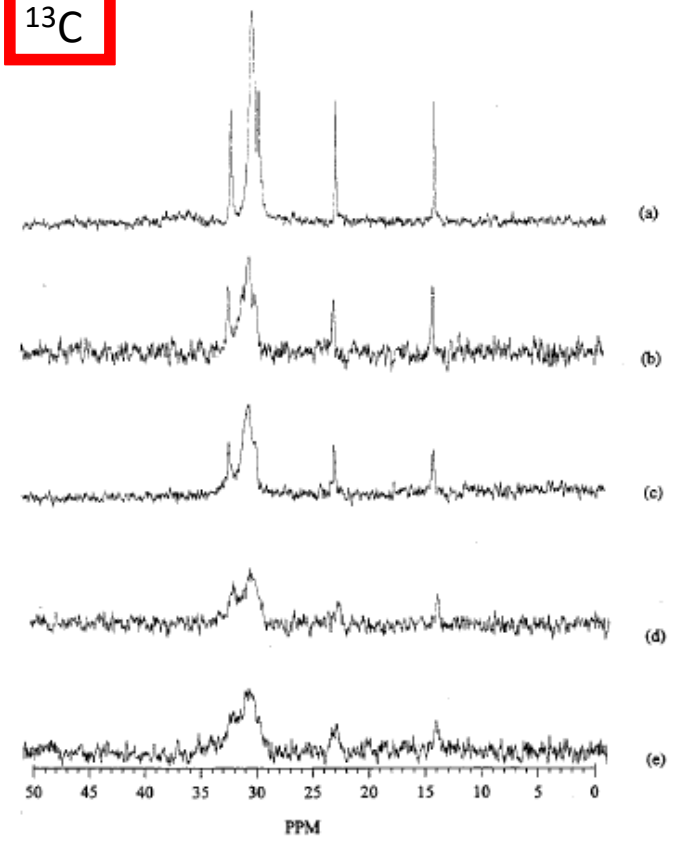

Figure 4. The ^{13}C NMR spectra (C_6D_6) of dodecanethiolate-protected Au clusters. Each spectrum was Fourier transformed using a line broadening of 3 Hz: (a) (−78°,2X,sd); (b) (90°,2X,sd); (c) (RT,1/3X,fd); (d) (RT,1/4X,fd); (e) (RT,1/6X,fd).

UV-Vis spectroscopy

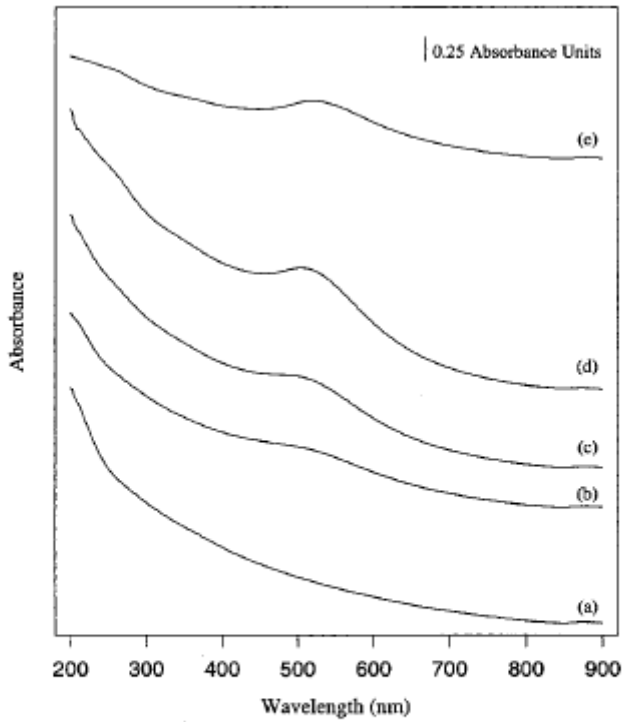

Figure 7. The UV/vis spectra (hexane) of dodecanethiolate-protected Au clusters: (a) (−78°,2X,sd), C = 3 × 10^{-6} M, MW = 3.4 × 10^4 amu; (b) (90°,2X,sd), C = 2 × 10^{-6} M, MW = 5.5 × 10^4 amu; (c) (RT,1/3X,fd), C = 4 × 10^{-7} M, MW = 2.3 × 10^5 amu; (d) (RT,1/4X,fd), C = 2 × 10^{-7} M, MW = 5.5 × 10^5 amu; (e) (RT,1/12X,fd), C = 9 × 10^{-8} M, MW = 1.1 × 10^6 amu.

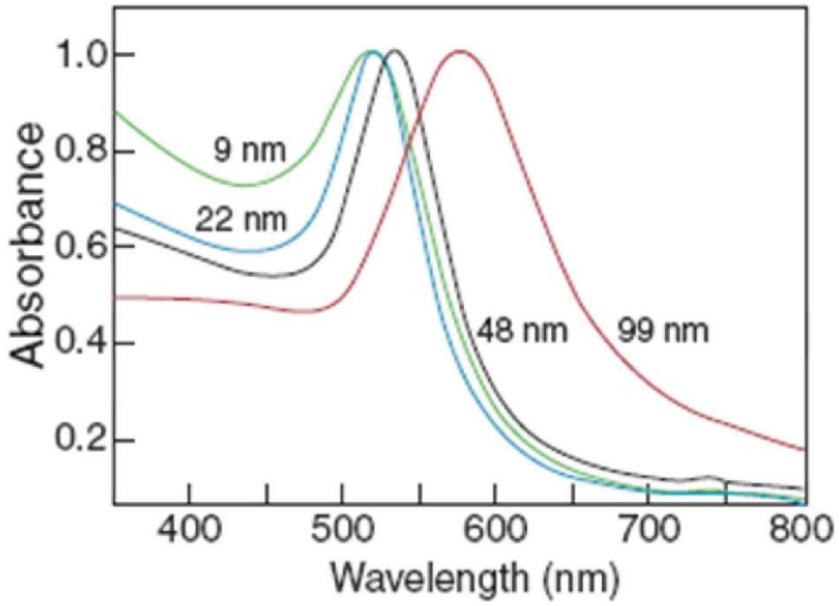

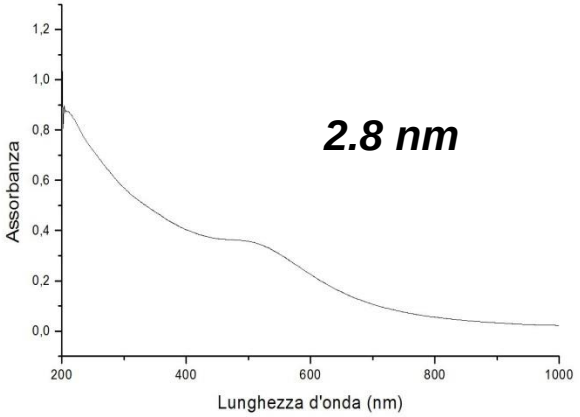

2.8 nm

MPC-C12

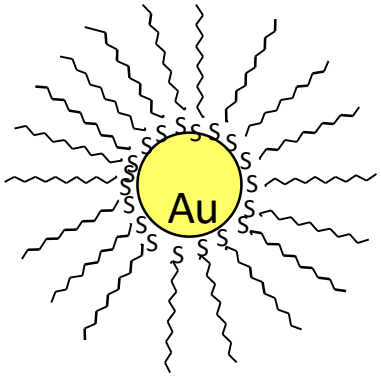

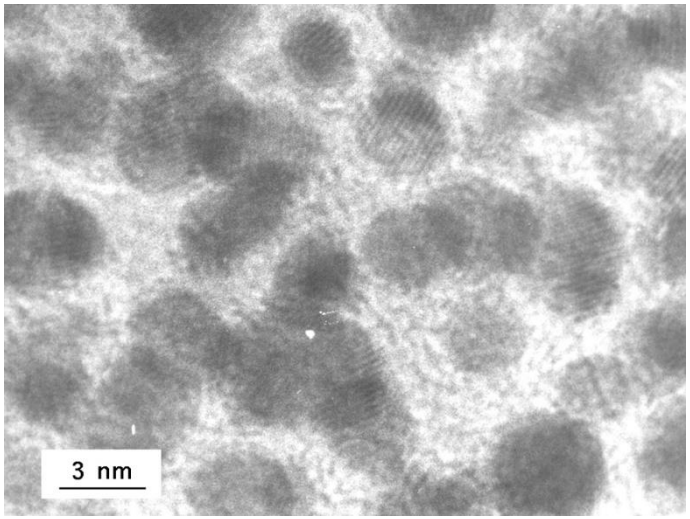

HRTEM

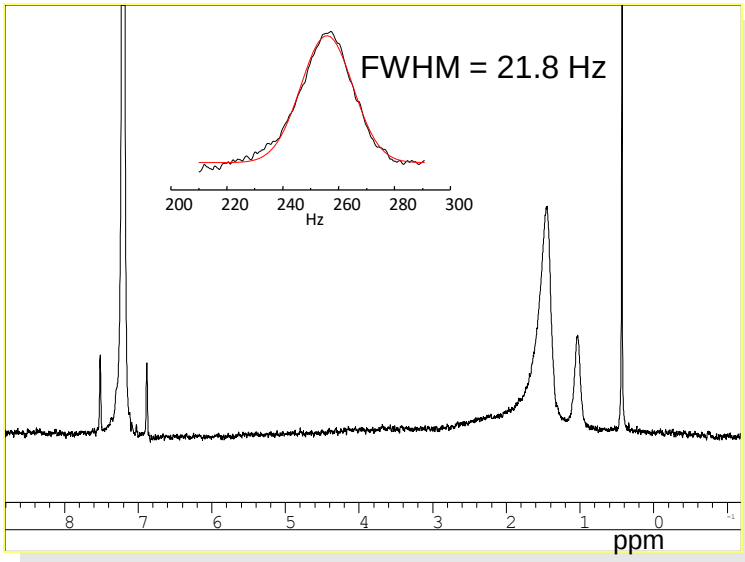

^{1}H NMR (250 MHz, C_6D_6)

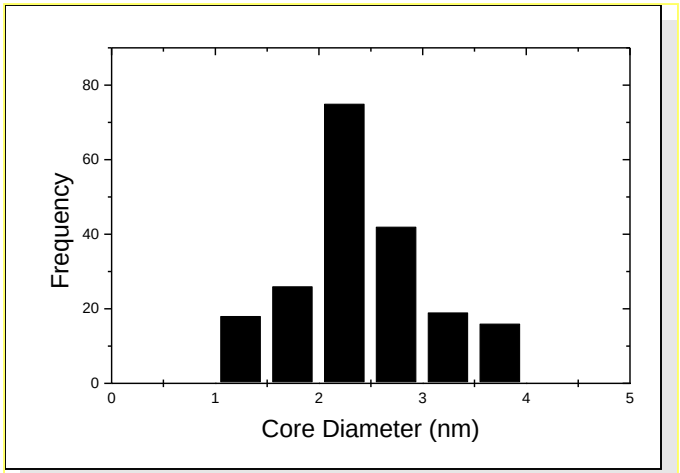

Core size histogram: core diameter 2.2 ± 0.4 nm

MPC-C12

$Au_{116}(SR)_{50}$ (MW=)

MPC-C12 - TGA Analysis

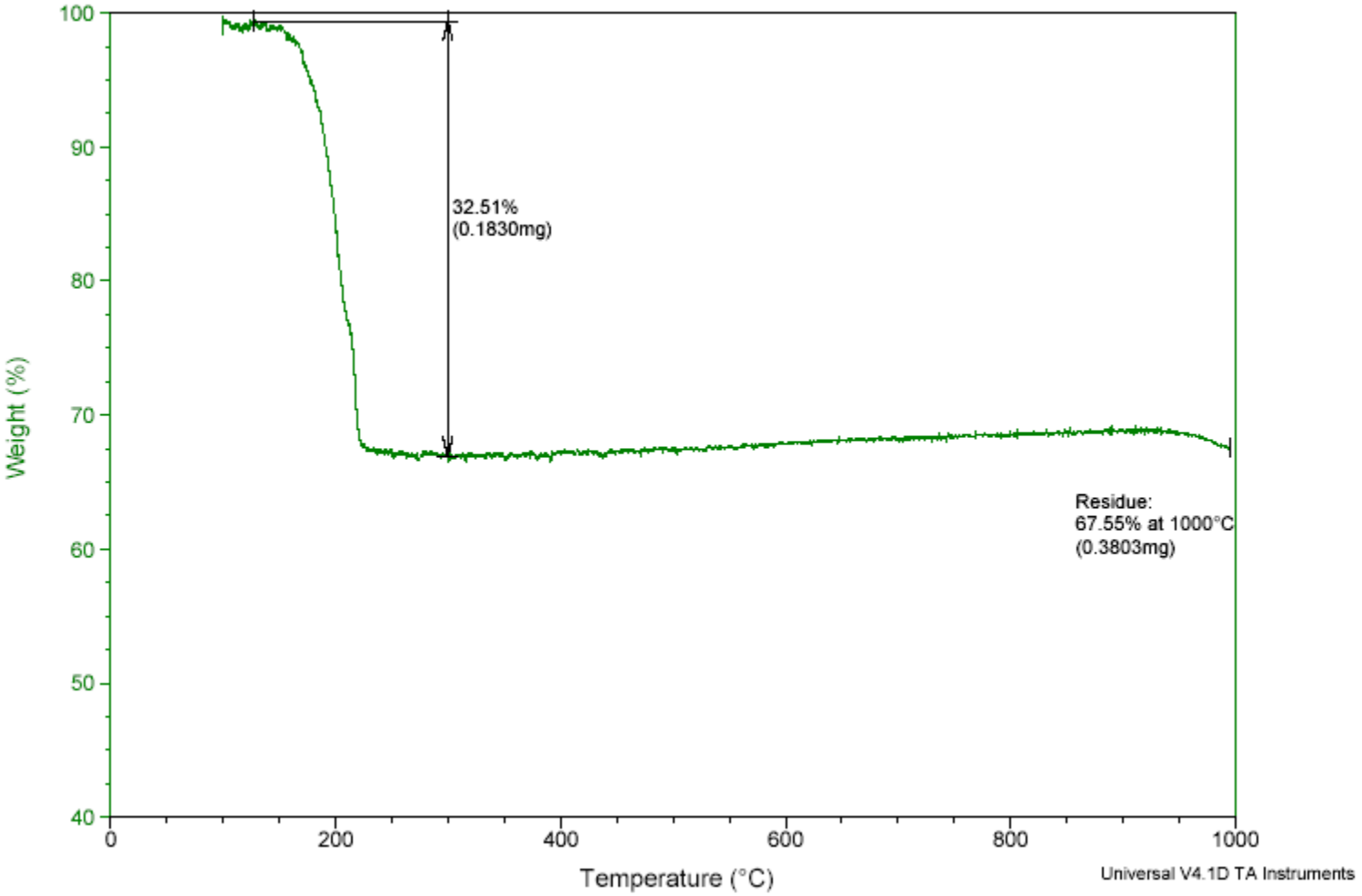

gold nanoparticles protected by a self-assembled organic layer

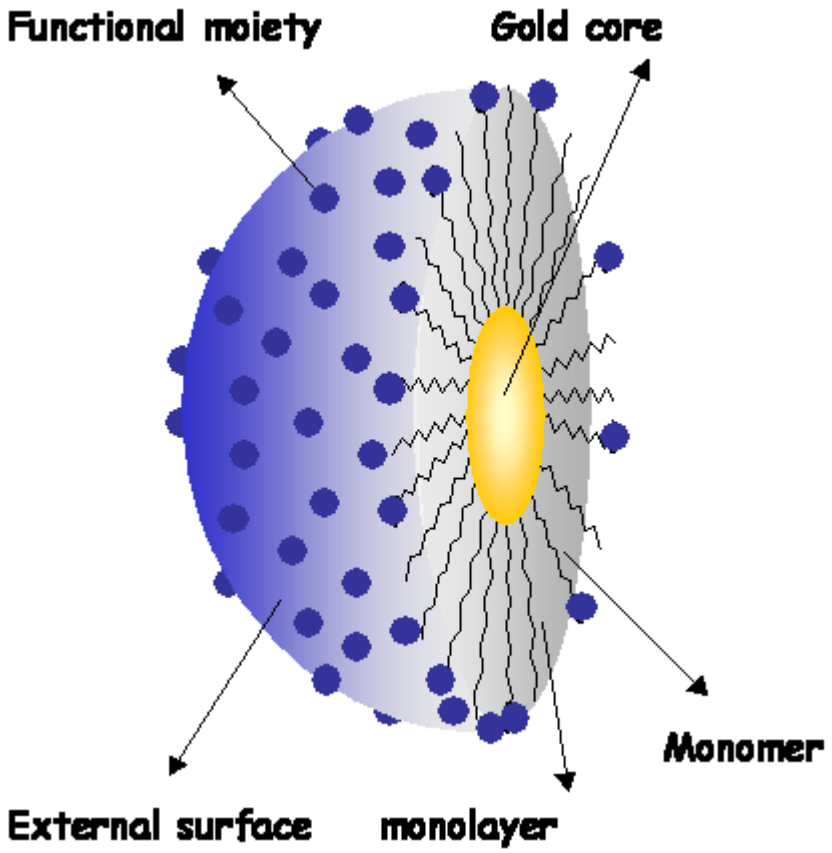

the metal core

✓ the size of the metal core determines the optical and elctronic properties

✓ the reaction conditions enable to tune the size, the shape and the dispersion

the self-assembled monolayer

✓ it is formed by a self-assembly process

✓ it is responsible for the stability

the solubility

the interaction with the environment

the function of the NP

water soluble nanoparticles

tiopronin

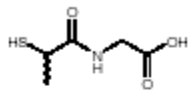

11

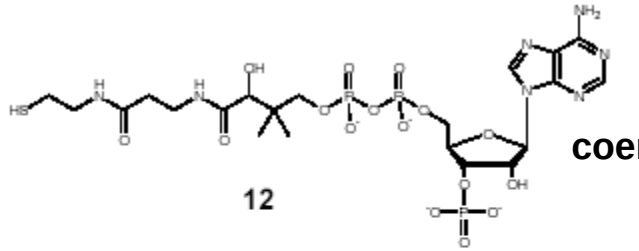

coenzyme A

12

13

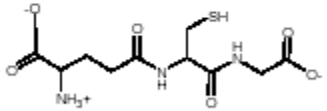

14 glutathione

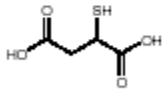

15

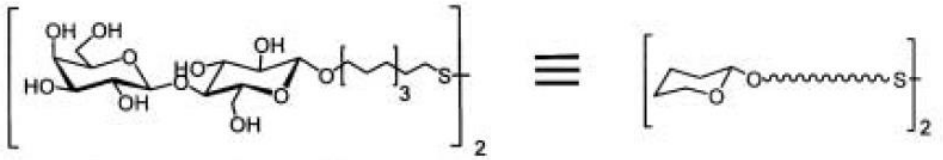

Lactose neoglycoconjugate

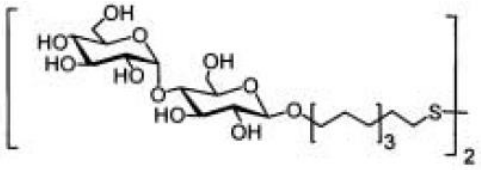

Maltose neoglycoconjugate

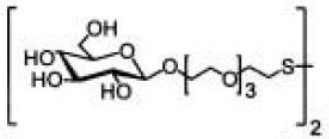

Glucose neoglycoconjugate

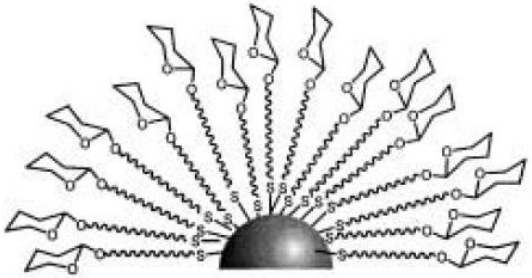

lacto-GNP
malto-GNP
gluco-GNP

water soluble nanoparticles

$PEG_{5000}SH$

21

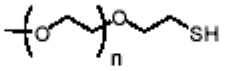

22a n = 1
22b n = 2
22c n = 3

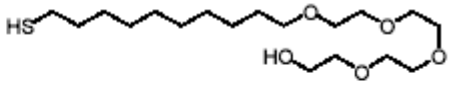

23

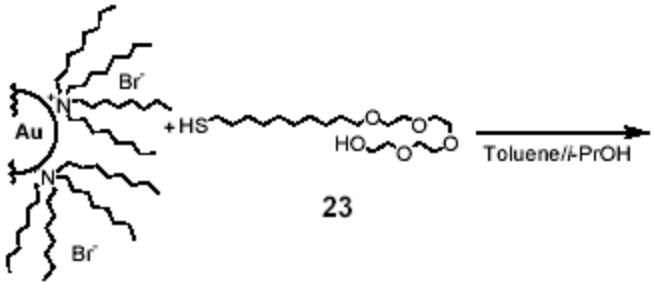

25 + 23 → Toluene/*i*-PrOH

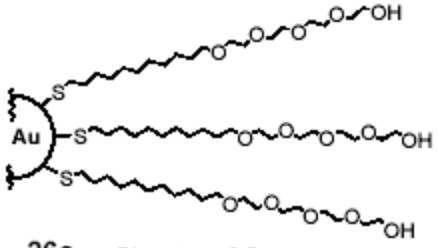

26a Diametro > 3.5 nm

$HAuCl_4$ + HS + 23 → $NaBH_4$ MeOH, HAc, *i*-PrOH

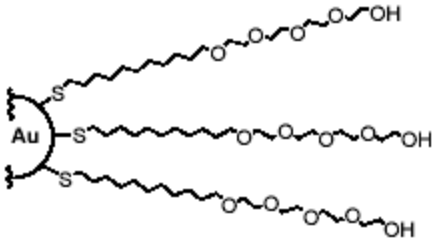

26b Diametro < 3.5 nm

water soluble nanoparticles

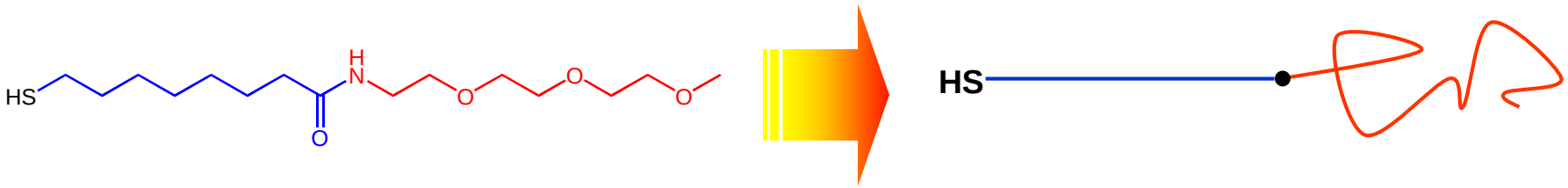

The hydrocarbon chain ensures the formation of a compact and tidy monolayer near the surface of the nanoparticle metal core

The polyether chain, even of short length, ensures MPCs solubility in water and polar solvents

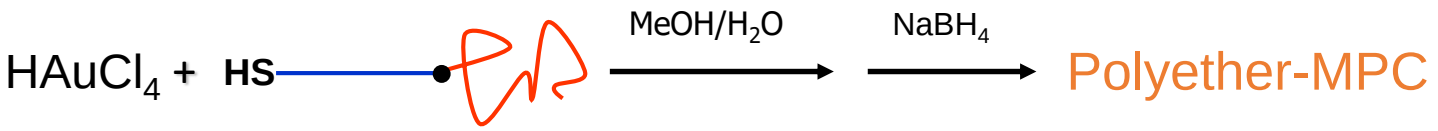

Homogeneous phase synthesis

Quantitative conversion of $HAuCl_4$

Diameter of the gold core 1.5 - 4.2 nm

Strong influence of the reduction rate

Pengo, P; Polizzi, S.; Battagliarin, M.; Pasquato, L.; Scrimin, P. *J. Mater. Chem.* **2003**, *13*, 2471-2478.

Thiolate Ligands for Synthesis of Water-Soluble Gold Clusters

C. J. Ackerson, P. D. Jadzinsky, R. D. Kornberg **J. AM. CHEM. SOC. 2005**, 127, 6550-6551

Table 1. Water-Soluble Thiolates and Their Ability to Passivate Gold Clusters

compound name	published synthesis	diameter (nm)[k]	soluble product	stability	synthetic method[a]	behavior in HD–PAGE gel
3-mercaptopropionic acid	ref 21	undetermined[j]	yes	days to weeks	Brust	did not enter matrix in HD or LD−PAGE[i]
4-mercaptobutyric acid	no	4.0 ± 1.2	yes	weeks	Brust	not tested
3-mercapto-1,2-propanediol	ref 14[b]	4.7 ± 1.2	yes	days	Brust	single diffuse band in HD−PAGE
cysteine	ref 12[c]	1.6 ± 0.3	yes	days	Brust[f]	entered gel matrix as single band; stalled; single band in LD−PAGE
methionine	no	2.4 ± 1.0	yes	weeks	Hutchison	did not enter matrix in HD or LD−PAGE
thiomalate	ref 13[d]	2.1 ± 1.4	yes	weeks	Brust	single tight band surrounded by large halo
2-mercaptobenzoic acid	no	2.1 ± 0.9	yes	minutes	Brust	did not enter matrix in HD or LD−PAGE
3-mercaptobenzoic acid	no	1.6 ± 0.6	yes	days	Brust	did not enter matrix; single band in LD−PAGE
4-mercaptobenzoic acid	ref 7[e]	1.8 ± 0.4	yes	months	Brust	2 tight bands
tiopronin	ref 9	1.9 ± 0.7	yes	months	Brust[f]	single diffuse pink band in HD or LD−PAGE
selenomethionine	no	1.6 ± 0.4	yes	days	Hutchison	did not enter matrix in HD or LD−PAGE
1-thio-β-D-glucose	no	2.1 ± 0.5	yes[g]	months	Brust[f]	single band in LD−PAGE
glutathione	ref 8	1.4 ± 0.4	yes	months	Brust	5 bands
ITCAE pentapeptide[h]	no	1.4 ± 0.4	yes	days	Hutchison	not tested

[a] Brust synthesis was in 1:1 water:methanol with a 3:1 thiolate:gold ratio. Typical concentrations were 10 mM gold and 30 mM thiolate. A 5-fold molar excess of $NaBH_4$ in a volume of water ~10% of the reaction volume was added to complete the cluster formation. Reactions denoted Hutchison were performed as described (ref 5). [b] A 1:1 ratio of thiolate:Au(III) and a 9-fold BH_4^- excess. [c] Cystine was used as the starting material to create cysteine MPCs. [d] Highest organothiolate:Au(III) ratio used was 5:2, with equimolar $NaBH_4$ to $HAuCl_4$, likely resulting in incomplete reduction. [e] A 1.8:1 thiolate:Au(III) ratio was used. [f] These compounds failed to form soluble products in 1:1 water:methanol, but did so under similar conditions in 6:1 methanol:acetic acid. [g] This compound formed product that remained in suspension following low-speed centrifugation, indicating cluster formation, but failed to redissolve after methanol precipitation; this product was not repeatably precipitable in methanol, but could be purified from starting materials by gel filtration and, otherwise, behaved as a stable water-soluble MPC. [h] The pentapeptide had the sequence Ile-Thr-Cys-Ala-Glu. [i] LD−PAGE was a standard 12% SDS−PAGE gel. [j] Particles form aggregates within which individual particle diameters cannot be measured. [k] See Supporting Information for images, histograms, and further analysis.

1. morphology is relevant

From Nature .....

- **Janus-like structures**

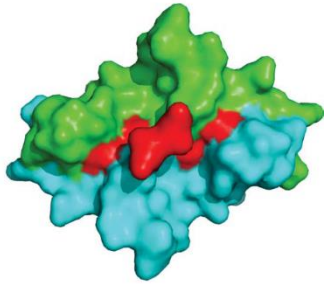

Heme dimer

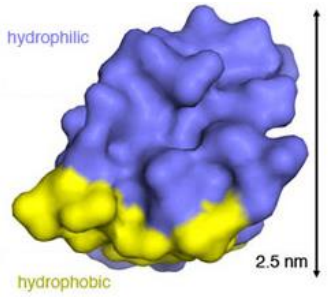

Hydrophobin

J. Rouvinen *J. Biol. Chem.* **2004**, *279* 527.

- **Patches-like systems**

Indian mallow pollen grain

M. Oeggerli, http://ngm.nationalgeographic.com/2009/12/pollen/oeggerli-photography, 2009

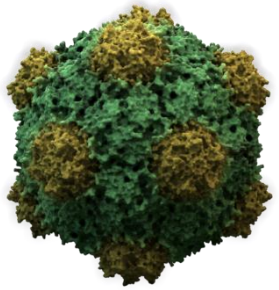

Cowpea Mosaic Virus

Thomas Splettstoesser (www.scistyle.com)

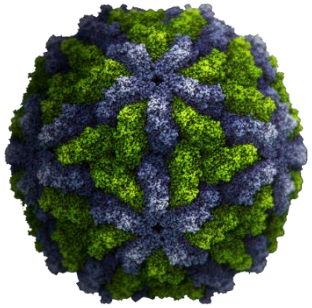

yellow fever virus

www.bianoti.com

2. ligand packing is relevant

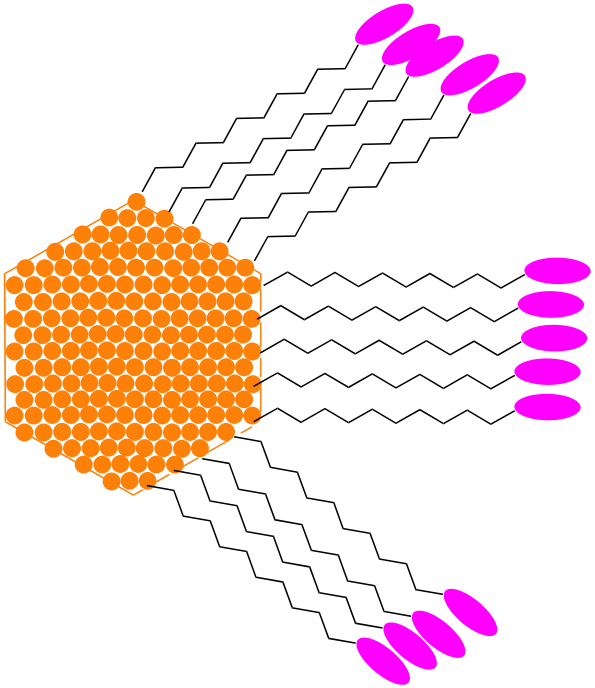

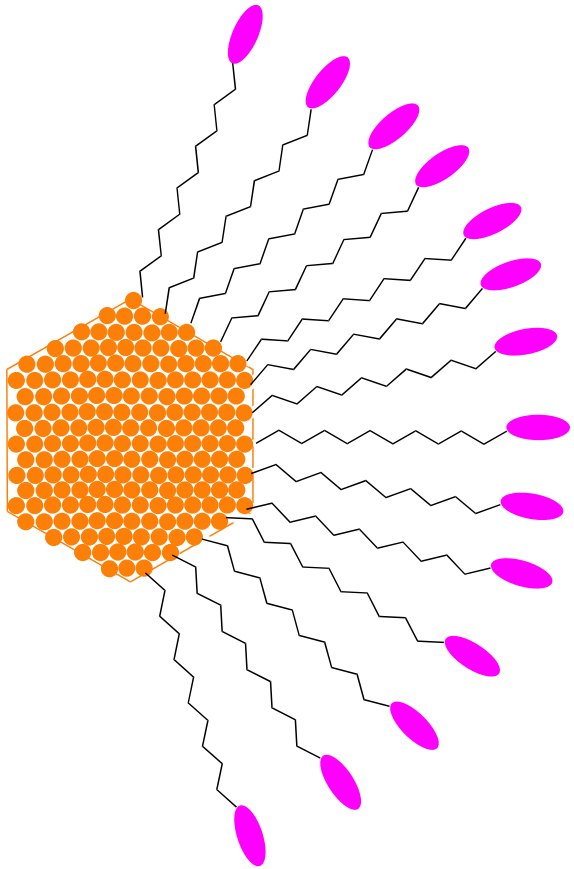

- maximize VdW interactions, and eventual week interactions among FG
- complex interfaces

- may prevent electrostatic repulsion among charged FG
- reduced VdW interactions
- may offers a better protection of Au surface
- one «sferical» interface

Monolayer packing

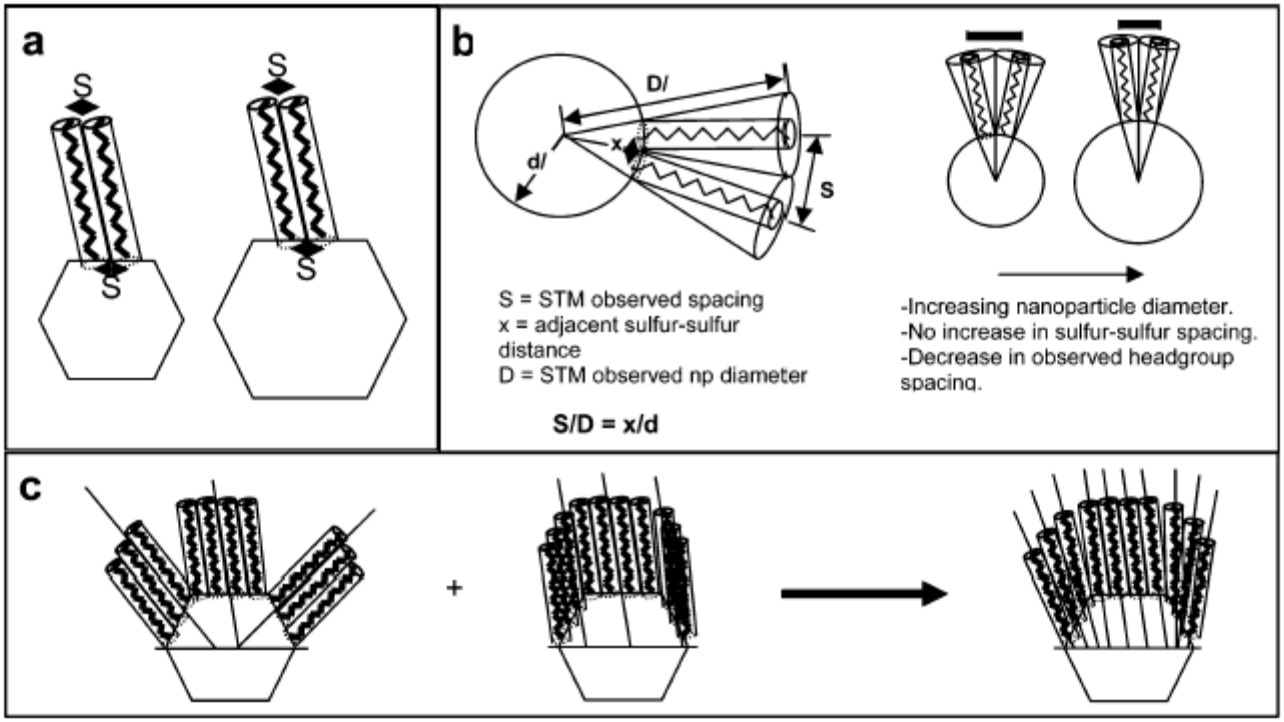

Figure 16. (a) Simplest representation of ligand packing for homoligand nanoparticles. Ligands pack on each nanoparticle facet as they would on a crystallographically equivalent flat 2-D gold surface, with a headgroup spacing corresponding exactly to the sulfur−sulfur spacing of the ligands at the nanoparticle core. (b) Schematic illustration of a ligand-coated nanoparticle relating the STM-observed headgroup spacing (S) at the periphery to the corresponding sulfur−sulfur spacing (x) at the nanoparticle core. (c) Ligands have essentially two configurations that they can assume on the faceted core: (i) they can assume their optimal tilt angle with regard to each facet (left), or (ii) they can assume a global tilt angle (middle). The first configuration leads to high-energy defects at the crystal edges, while the second does not take advantage of the particle curvature. Hence, the true configuration is likely a compromise between the two, with the ligands roughly conforming to a global tilt angle, but relaxing, and splaying outward as shown in the rightmost drawing in (c).

F. Stellacci et al. *J. AM. CHEM. SOC.* **2006**, *128*, 11135-11149.

Properties of the Monolayer

EPR Spectroscopy as a tool to investigate the monolayer properties

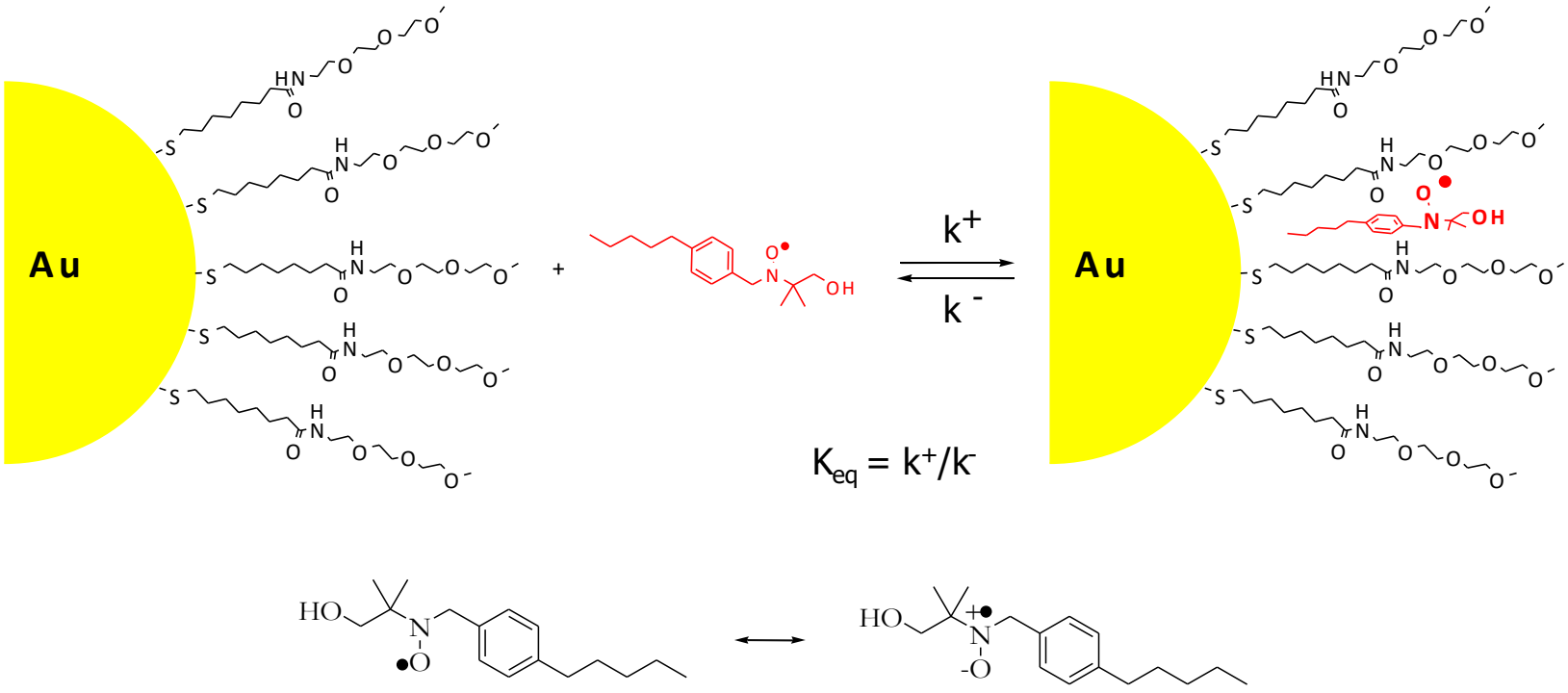

- the hyperfin coupling constants *a*(N) and *a*($2H_\beta$) are larger in polar media

M. Lucarini, P. Franchi, G. F. Peduli, P. Pengo, P. Scrimin, L. Pasquato, *J. Am. Chem. Soc.*, **2004**, *126*, 9326.

Properties of the Monolayer

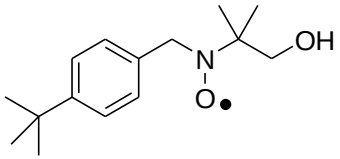

$1 \div 2 \times 10^{-5}$ M

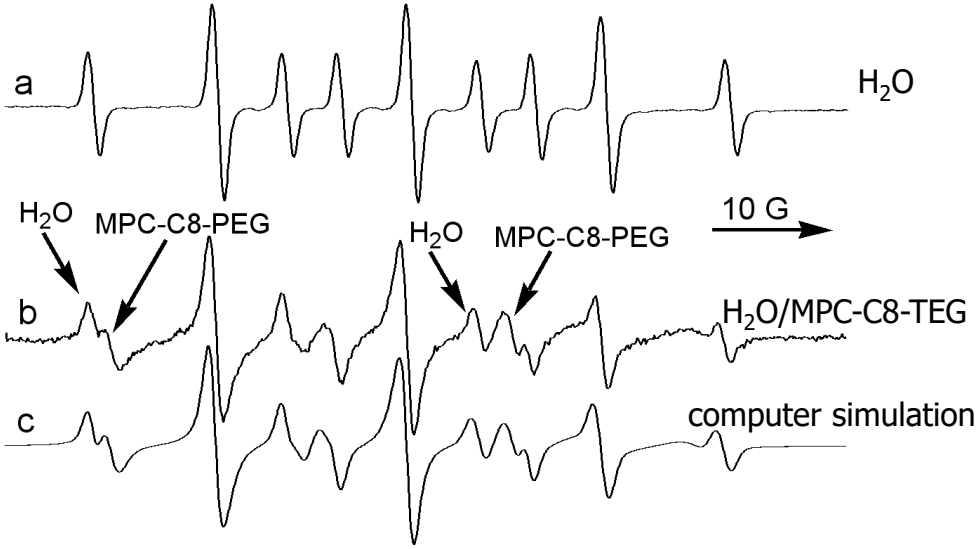

k^+ 7.7 10^9 $M^{-1}s^{-1}$

k^- 1.9 10^6 s^{-1}

K_{eq} 5.683 M^{-1}

MPC-C8-TEG, d = 3.4 nm, σ 0.7 nm

rapid exchange of the probe between the aqueous phase and the monolayer

the nitroxide group is located in a less polar environment shielded from the aqueous solvent

M. Lucarini, P. Franchi, G. F. Peduli, P. Pengo, P. Scrimin, L. Pasquato, *J. Am. Chem. Soc.*, **2004**, *126*, 9326.

Monolayer packing

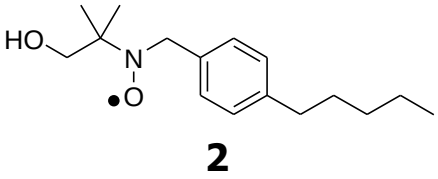

2

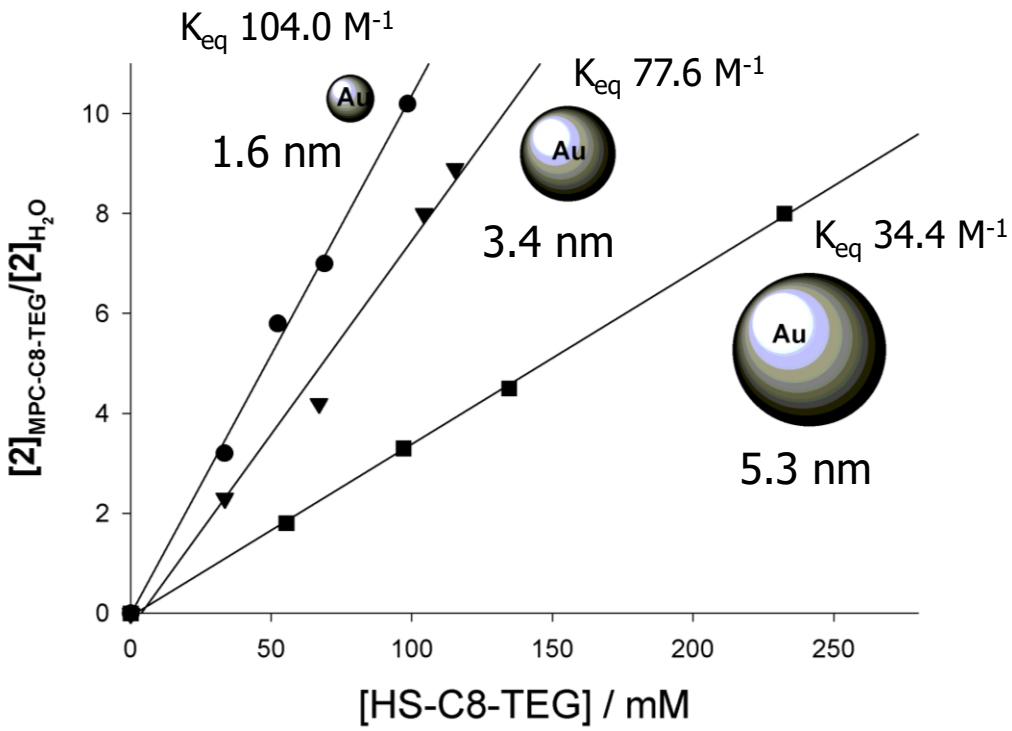

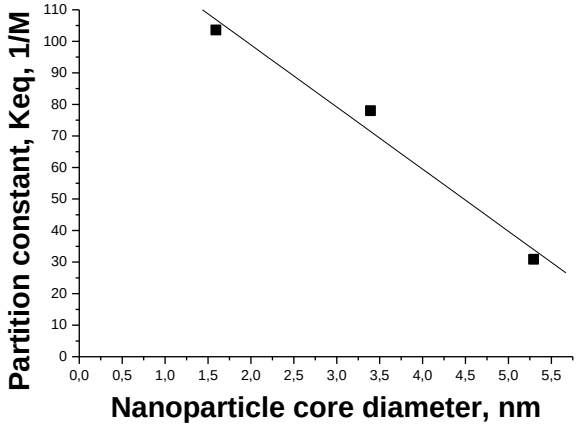

M. Lucarini, P. Franchi, G. F. Pedulli, C. Gentilini, S. Polizzi, P. Pengo, P. Scrimin, L. Pasquato, *J. Am. Chem. Soc.* **2005**, *127*, 16384.

Monolayer packing

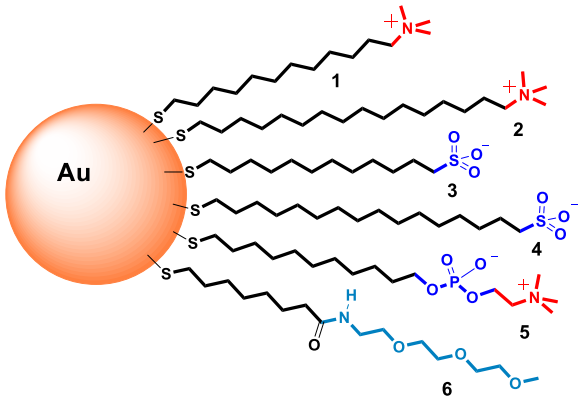

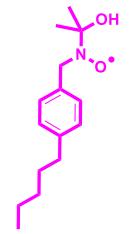

radical probe

Table 1. Spectroscopic parameters for the radical probe and partition equilibrium (K_{eq}) constants.

NP	T (K)	a_N (G)	a_{2H} (G)	K_{eq} (M^{-1})
-	300	16.25	10.14	
-	340	16.22	9.80	
NP-1	300	15.20	8.50	131
NP-1	340	15.35	8.46	20
NP-2	300	14.50[a]	8.45[a]	
		15.18	8.58	
NP-2	340	15.15	8.50	320
NP-3	300	15.15	8.40	133
NP-3	340	15.40	8.48	26
NP-4	300	14.40[a]	8.38[a]	
		15.23	8.30	
NP-4	330	14.58[a]	8.40[a]	
		15.33	8.33	
NP-4	340	15.32	8.40	98
NP-5	300	15.25	8.35	550
NP-6[b]	298	15.70	9.00	77

M. Lucarini, P. Posocco, L. Pasquato et al. J. Coll. Interf. Sci. **2022**, 607, 1373.

Monolayer packing

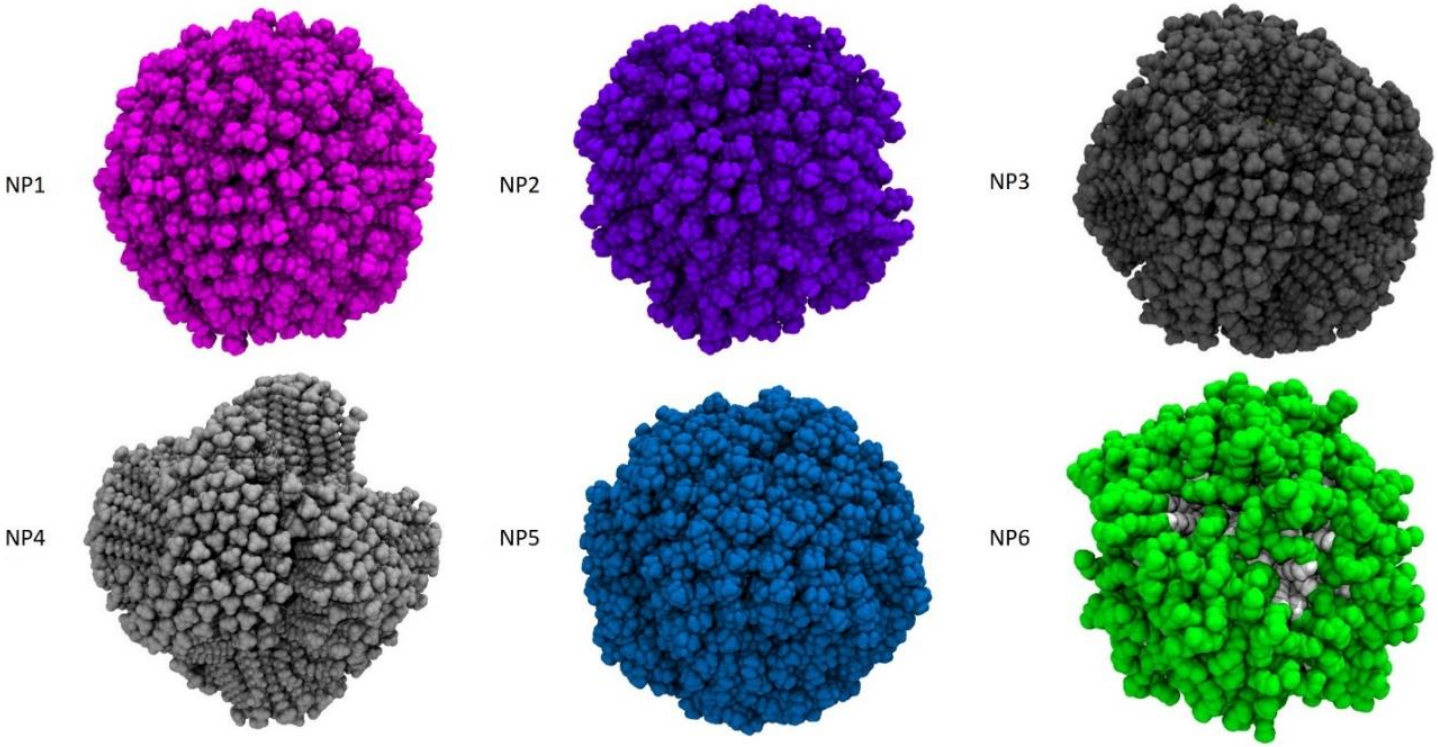

M. Lucarini, P. Posocco, L. Pasquato et al. J. Coll. Interf. Sci. **2022**, 607, 1373.

Monolayer packing

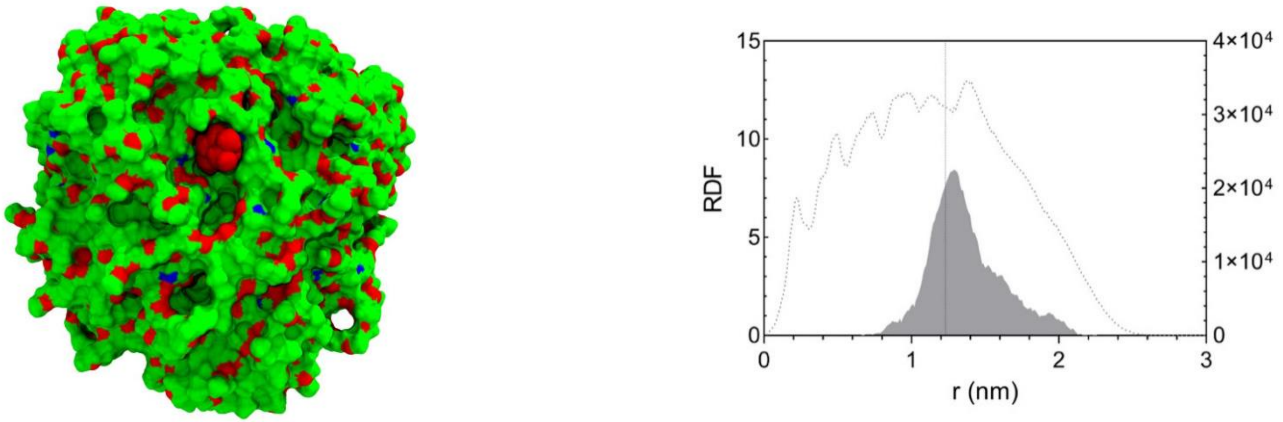

Figure S2. a) Binding of the radical probe (in red) within **NP6**. Solvent is omitted for clarity, oxygen atoms are in red and nitrogen atoms in blue, all the others atoms of the ligand are in green.
b) Radial distribution function (RDF) of nitrogen atom of the radical probe (solid line, left axis) and thiolate of **6** (dotted line, right axis) reported from the gold surface

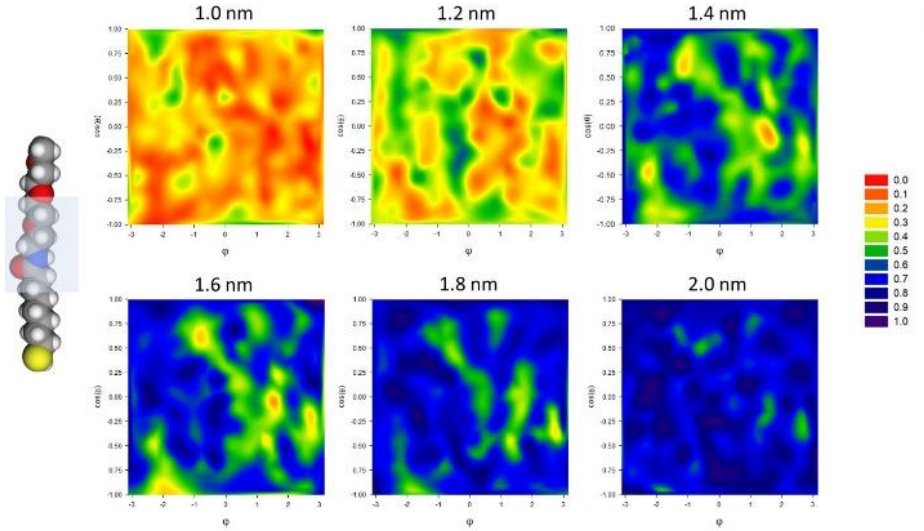

M. Lucarini, P. Posocco, L. Pasquato et al. J. Coll. Interf. Sci. **2022**, 607, 1373.

Monolayer packing

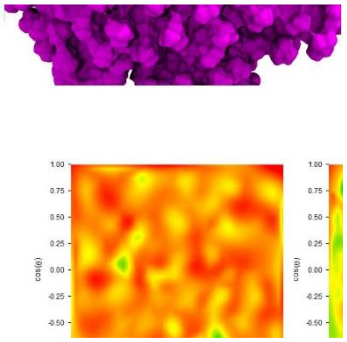

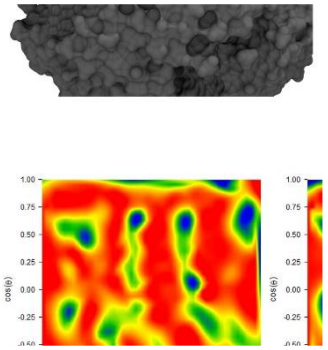

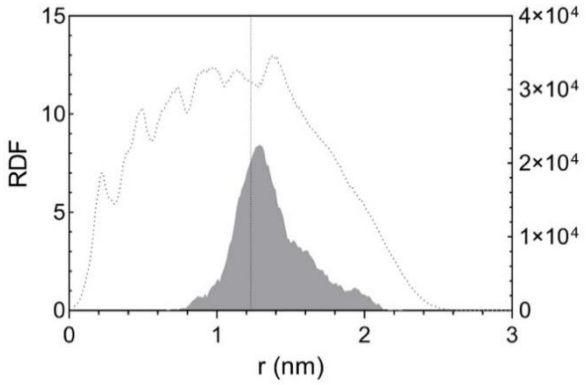

NP1

NP3

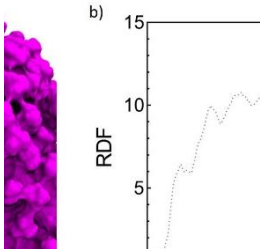

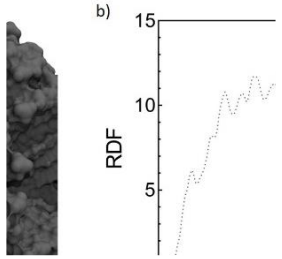

M. Lucarini, P. Posocco, L. Pasquato et al. J. Coll. Interf. Sci. **2022**, 607, 1373.

Monolayer packing

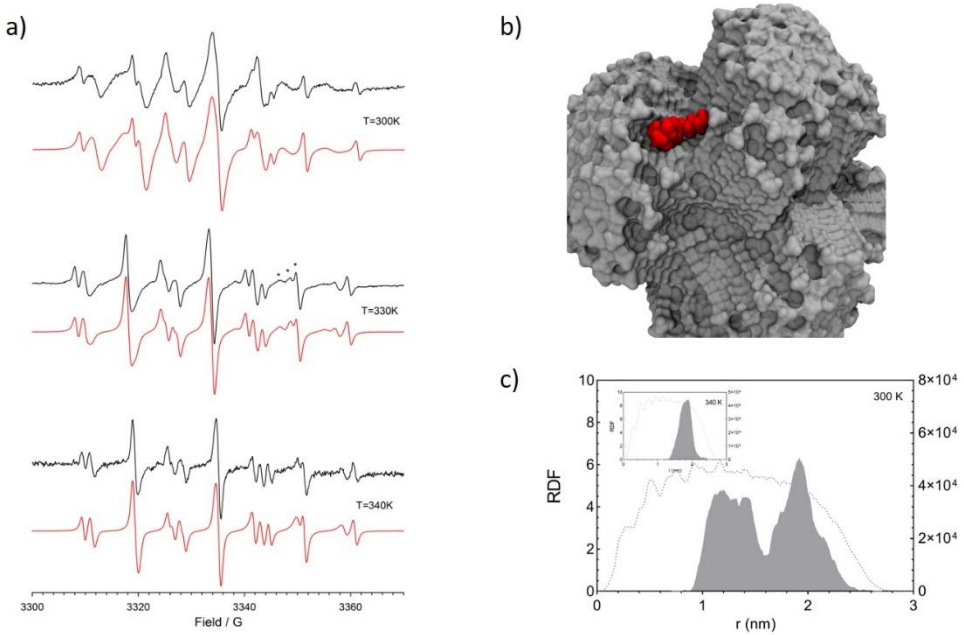

Figure 5. a) EPR spectra of the radical probe recorded in the presence of **NP4** (13.3 mg/0.1mL) at 300 K (top), 330 K (middle) and 340 K (bottom). Stars refer to the three different radical species (see text). In red are reported the corresponding theoretical simulations; b) Binding of the radical probe (in red) within **NP4**. Solvent is omitted for clarity. c) Radial distribution function (RDF) of nitrogen atom of the radical probe in the monolayer of **NP2** (solid line, left axis) and ligand **2** (dotted line, right axis) reported from the gold surface. Insert: same RDFs as in panel c), but predicted at 340 K.

M. Lucarini, P. Posocco, L. Pasquato et al. J. Coll. Interf. Sci. **2022**, 607, 1373.

Monolayer packing

Dynamics of Thiolate Chains on a Gold Nanoparticle

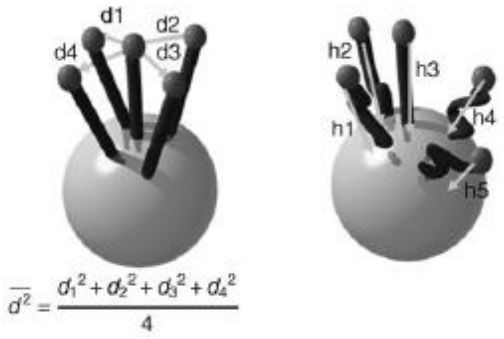

Figure 2. Cartoons illustrating how terminal chain atoms become more available to the external environment. Left: increase of the "horizontal" distance from the neighbors. Right: increase of the height from the particle surface.

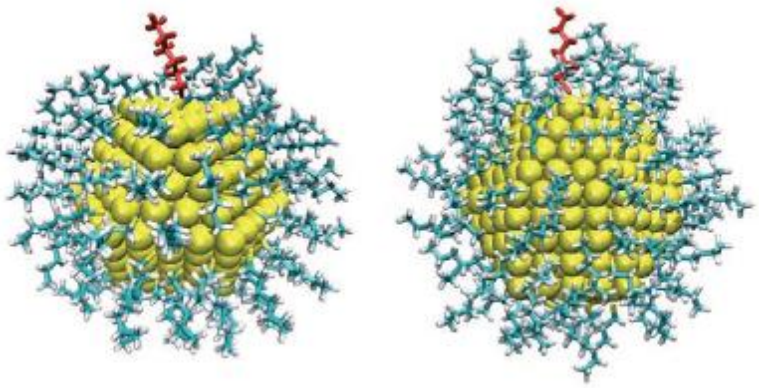

$Au_{309}(SC_6H_{13})_{80}$

diametro 2.3 nm

shape: CO

Figure 4. Schematic representation of the molecular-dynamics simulations. The red thiolate represents the least crowded (left) and the most linearly extended (right) thiolate.

S. Rapino and F. Zerbetto, *Small,* 2007, **3**, 386-388.